

# Synthesis of chlorins and bacteriochlorins from cycloaddition reactions with porphyrins

Nuno M. M. Moura,\* Carlos J. P. Monteiro, Augusto C. Tomé, M. Graça P. M. S. Neves,  
and José A. S. Cavaleiro\*

LAQV-REQUIMTE, Chemistry Department, University of Aveiro, 3810-193 Aveiro, Portugal

Email: [nmoura@ua.pt](mailto:nmoura@ua.pt) and [jcavaleiro@ua.pt](mailto:jcavaleiro@ua.pt)

Dedicated to Prof. Girolamo Cirrincione in recognition of his outstanding organic and medicinal chemistry contributions, on the occasion of his university retirement

Received mm-dd-yyyy

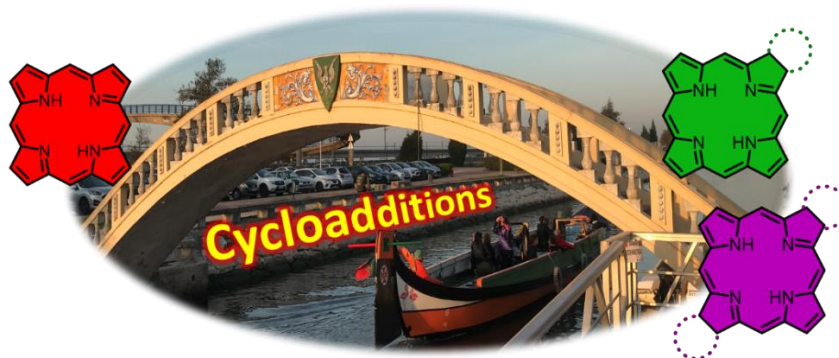
Accepted mm-dd-yyyy

Published on line mm-dd-yyyy

Dates to be inserted by editorial office

## Abstract

Chlorins and bacteriochlorins are reduced porphyrin-type derivatives displaying characteristic structural, physical, and chemical features. Such features make chlorins and bacteriochlorins key “players” in several fields, and specifically in medicine as photosensitizers (PSs) for the diagnosis and treatment of neoplastic situations by photodynamic therapy. Cycloaddition approaches have become important synthetic tools to prepare chlorin and bacteriochlorin macrocycles. This review highlights the procedures developed over the last 10 years to synthesize chlorins and bacteriochlorins, namely through Diels–Alder and 1,3-dipolar reactions using porphyrin macrocycles as templates.



**Keywords:** Porphyrinoids, chlorins, bacteriochlorins, cycloaddition reactions, Diels–Alder, 1,3-dipolar cycloaddition

## Table of Contents

1. Introduction
  2. Diels–Alder reactions
    - 2.1 Vinyl-substituted porphyrins as dienes
    - 2.2 Porphyrins as dienophiles
  3. 1,3-Dipolar cycloadditions
    - 3.1 Reaction of porphyrins with azomethine ylides
    - 3.2 Reaction of porphyrins with nitrile oxides
    - 3.3 Reaction of porphyrins with silyl nitronates
    - 3.4 Reaction of porphyrins with nitrones
    - 3.5 Reaction of porphyrins with nitrile imines
  4. Other cycloadditions
  5. Porphyrinoids cycloaddition reactions
  6. Conclusions
- Acknowledgements
- References

## 1. Introduction

Life on Earth would not exist as it is happening if natural processes such as respiration and photosynthesis would not be taking place. Porphyrin derivatives play a key role in such processes. Particularly in photosynthesis, the so-called chlorophylls are the most significant “actors”. This vital biological action has attracted the attention of many scientists along the centuries. In relation with this interest in understanding Nature and its events, many references can be put forward. Let us consider only three of such references which are specifically related to the scientists’ search for knowledge. One of them appeared in 1614 and was due to Sir Walter Raleigh in his “History of the World: Preface” (Man cannot give a true reason for the grass under his feet, why it should be green rather than red or any other color).<sup>1</sup> Another reference was published in 1906 by Willstätter and relates the results obtained on the composition of chlorophyll,<sup>2</sup> and the third one, a communication on the synthesis of chlorophyll *a* was published in 1960 by Woodward and 17 collaborators.<sup>3</sup> Interestingly, thirty years later the full synthetic methodology related to the contents of that communication was published by the same authors.<sup>4</sup> The macrocycles of such compounds, in comparison with those of porphyrins, contain one reduced pyrrolic unit and so are dihydroporphyrin derivatives. All natural and synthetic compounds containing macrocycles of that type are called chlorins. In such way, the following question “How would be the life on Earth without the natural chlorins?” can be wavering in the mind of any human being.

There are other natural compounds named bacteriochlorophylls which occur in phototropic bacteria.<sup>5</sup> Some of such compounds contain tetrahydro-type porphyrin macrocycles with two reduced pyrrole rings at opposite positions. Other derivatives isolated from bacterial enzymes contain two reduced pyrrole rings at adjacent positions and these are called isobacteriochlorins (Figure 1).

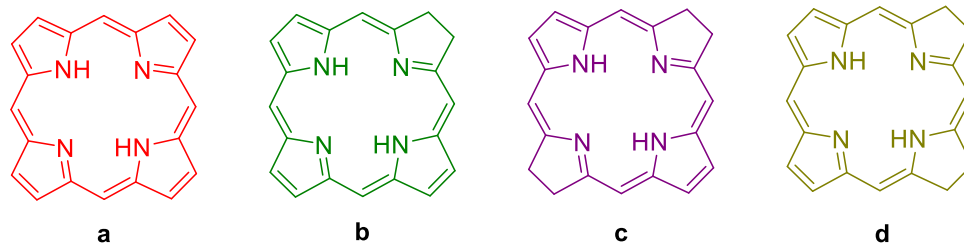


**Figure 1.** Structures of Porphyrin (a), Chlorin (b), Bacteriochlorin (c) and Isobacteriochlorin (d).

The vital functions played by such natural porphyrin derivatives certainly brought the motivation of many scientists to understand their synthesis and biosynthesis, mode of action and metabolism. That led to many studies and publications in the last century and synthetic routes for a significant variety of porphyrinoids and their potential applications have been put forward.<sup>6–10</sup> Using porphyrin derivatives obtained by simple and efficient synthetic methods, applications have been demonstrated in several areas such as catalysis, materials, and medicine. Other applications as anticancer and anti-microbial agents are also very significant for humankind. Photodynamic therapy requires a good photosensitizing (PS) action taking place after its administration, accumulation in cancer cells and irradiation with an adequate radiation ( $\lambda > 630$  nm).<sup>11</sup> The result is the formation of reactive oxygen species (mainly singlet oxygen and oxygen radicals) which bring death to the neoplastic cells. The absorption of radiation is then a key step in the process.<sup>12</sup> In this sense, chlorins<sup>13</sup> and bacteriochlorins<sup>14</sup> are better sensitizers than porphyrins and isobacteriochlorins, since the former have higher absorptions at higher wavelengths in a wavelength range of deeper radiation penetration.<sup>15</sup>

Certain chlorins and bacteriochlorins have already obtained medicinal approval and are being used in photodynamic therapy of cancer or are under clinical trials. Some examples will now be mentioned.

Foscan<sup>®</sup>, the brand name of Temoporfin, a chlorin derivative, is being used since 2001 for lung, brain, neck and head cancer types (Figure 2).<sup>16,17</sup>

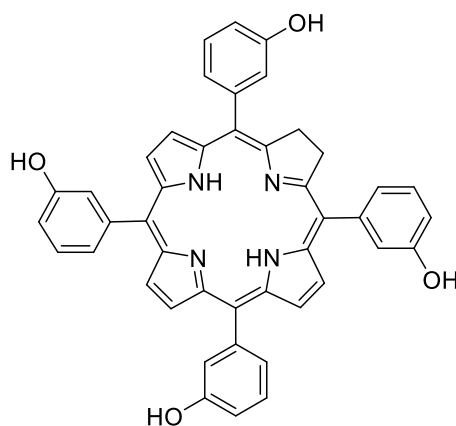


**Figure 2.** Temoporfin structure.

Visudyne<sup>®</sup>, the brand name of the chlorin derivative Verteporfin, formulated as a mixture of two isomers, is being used against age-related macular degeneration (Figure 3).<sup>17</sup>

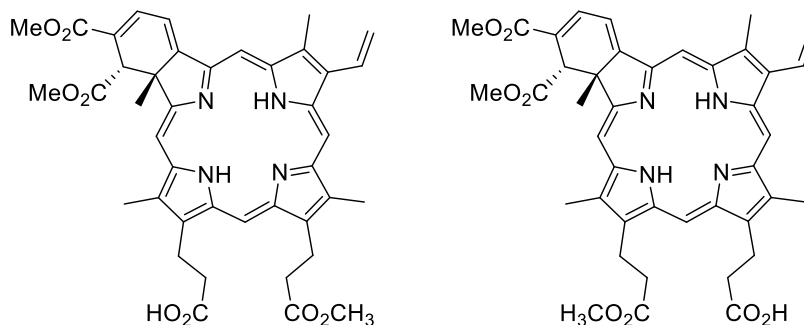


**Figure 3.** Structures of the two Verteporfin isomers.

In addition, other chlorin derivatives (*e.g.*, MACE, Photochlor) and bacteriochlorins (*e.g.*, Tookad) are still under clinical evaluation against several types of tumors (Figure 4).<sup>17–19</sup>

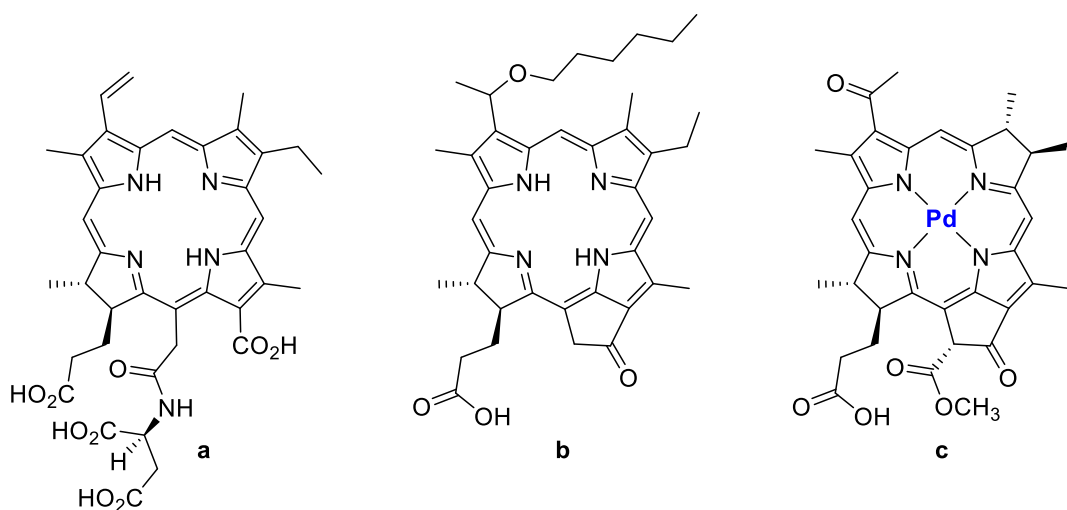


**Figure 4.** Structures of MACE (a), Photochlor (b) and Tookad (c).

The potential use in several fields, mainly those with biological significance, have been a driving force for studies having hydroporphyrins as targets. As a result, many publications and book series have been published on this subject. Keeping in mind the potential applications of chlorins and bacteriochlorins, and considering the great synthetic capabilities brought by cycloaddition transformations, this review will deal with literature publications which appeared in the last 10 years on the synthesis of such porphyrin derivatives by cycloaddition procedures, although older ones may also be considered for a better understanding. Considering the structural features of the porphyrin macrocycles under study, their reactions as dienes, or as dienophiles or dipolarophiles will thus be discussed in this review.

## 2. Diels–Alder reactions

### 2.1 Vinyl-substituted porphyrins as dienes

Almost at the same time, the groups of Johnson<sup>20</sup> and Inhoffen<sup>21</sup> have shown that protoporphyrin-IX (

Figure 5) can react in [4+2] cycloaddition processes with dienophiles like tetracyanoethylene (TCNE), dimethyl acetylenedicarboxylate (DMAD) or singlet oxygen. Chlorin-type compounds were the main products obtained

although in some cases the reactions gave mixtures of products, including chlorin, isobacteriochlorin, and other porphyrin-type derivatives.

During the last 10 years, interesting reviews covering the chlorins' chemistry and their potential applications have been published.<sup>13,22</sup> As far as the chlorins' synthesis is concerned, several publications are mentioned in such reviews, mainly those involving the [4+2] cycloadditions with  $\beta$ -vinylporphyrins.

Oliveira *et al.*<sup>13</sup> have reported a concise, but very informative, review related with the natural occurrence and physical-chemistry features of chlorophylls *a*, *b*, *d*, *f* (

Figure 5). Information on synthetic methods, including the cycloaddition features leading to chlorins, is included in the review, as well as their potential applications in cancer photodynamic therapy and diagnosis, catalysis, and in the materials area.

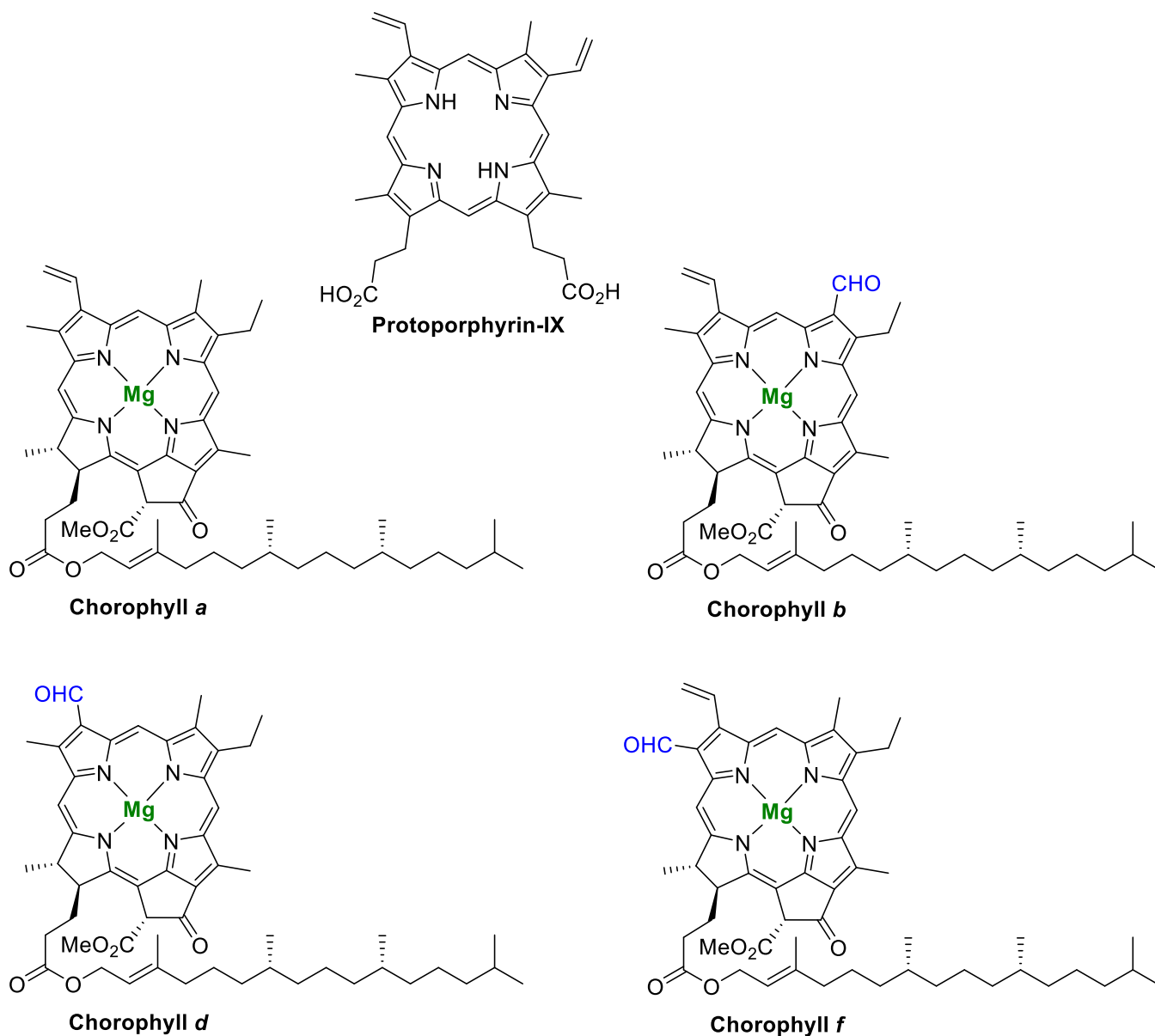
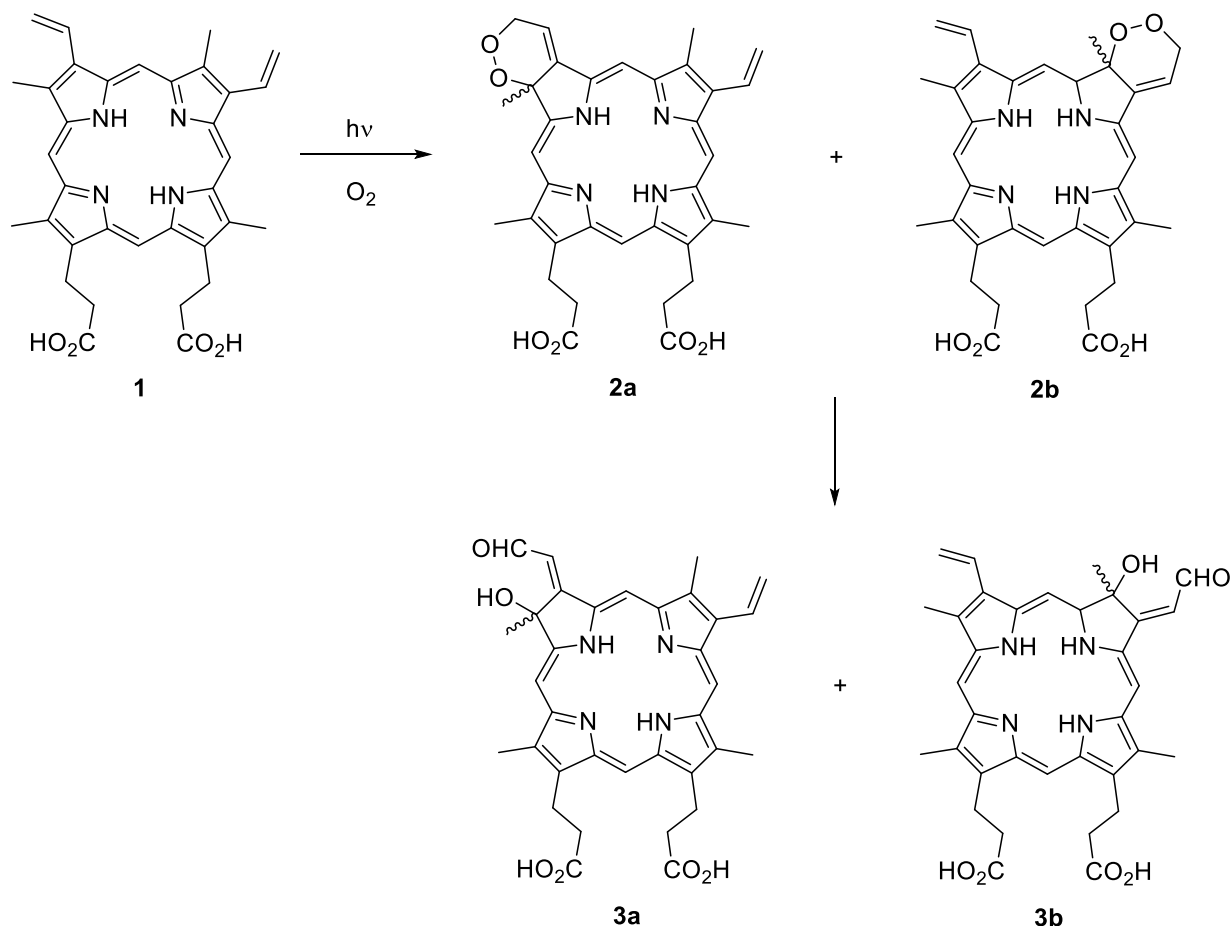


**Figure 5.** Structures of Protoporphyrin-IX and Chlorophylls *a*, *b*, *d* and *f*.

Taniguchi and Lindsey<sup>22</sup> have published an excellent review about synthetic chlorins obtained from the derivatization of porphyrins. It covers the “chlorin world” until six years ago. Synthetic methods to afford chlorin-type macrocycles are put forward and the synthesis of more than 1000 chlorins or related macrocycles is considered. Spectral features of chlorins and chlorophylls are also compared and the possibility of synthetic chlorins becoming surrogates for chlorophylls is also discussed.

As far as the cycloaddition approaches are concerned, it can be stated that a very good survey until 2015 is considered in that review. It starts with the cycloaddition behavior of vinylporphyrins in the presence of oxygen and light. With protoporphyrin-IX there is formation of two isomeric photoprotoporphyrins (**2a** and **2b**). The scission and rearrangement of the peroxy group in each compound leads to the formation of the corresponding isomeric chlorins **3a** and **3b** (Scheme 1). This method, leading to such chlorins and their protoporphyrin-IX precursors, was used in further studies carried out by several groups.<sup>21,23</sup>

The initial cycloaddition method with protoporphyrin derivatives and TCNE and DMAD was extended to other dienophiles like urazines, maleimides, 4-nitro-1-nitrosobenzene and others with electron-deficient features. Chlorins have been the main products from these experiments, although in some cases the bis-addition took place resulting in the formation of isobacteriochlorins.<sup>22,23</sup>



**Scheme 1.** Chlorin products from the reaction of protoporphyrin-IX with  $^1\text{O}_2$ .

Brückner *et al.* also have reviewed the synthetic procedures to bacteriochlorins and isobacteriochlorins.<sup>24</sup> It is clear that the main products in each Diels–Alder cycloaddition depends on the starting vinylporphyrin and its reactivity.

For example, a spiro[chlorin–porphyrin]-type dimer was readily prepared by heating the [tetra-( $\beta,\beta'$ -sulfoleno)porphyrinato]zinc(II) precursor in 1,2-dichlorobenzene at 140 °C for 2 h. The reaction underwent a [4+2] self-cycloaddition *via* a  $\beta,\beta'$ -bis(methylene)porphyrin intermediate generated *in situ* by thermal SO<sub>2</sub> extrusion, which in the absence of an added dienophile led to the formation of the spiro(chlorin–porphyrin zinc(II) complex **4** (Figure 6).<sup>25</sup>

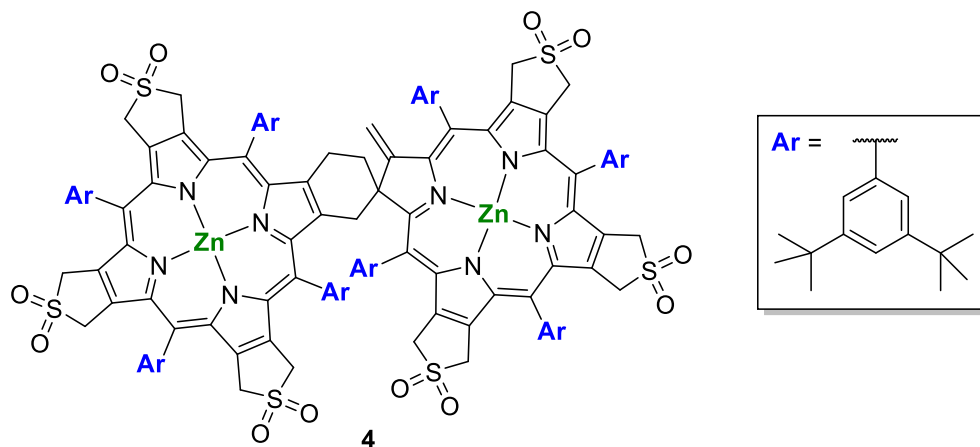


**Figure 6.** Structure of the spiro(chlorin–porphyrin) **4**.

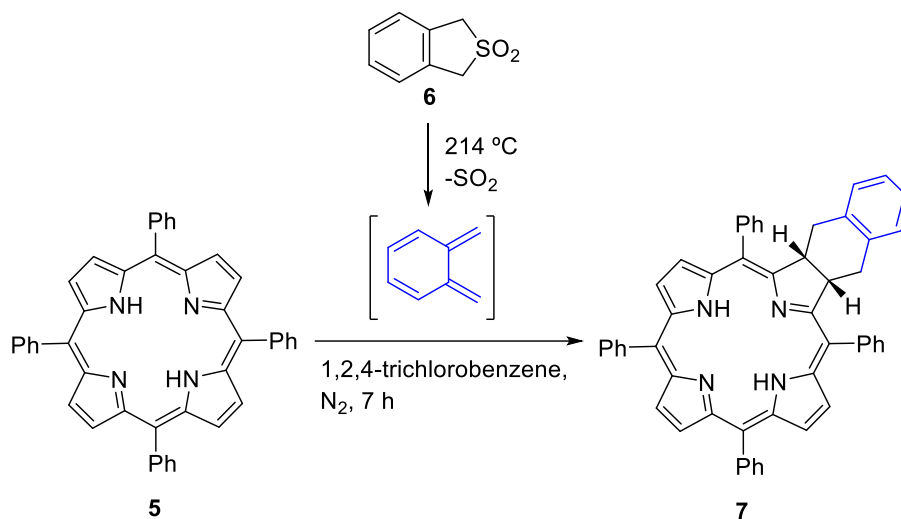
## 2.2 Porphyrins as dienophiles

The transformation of a porphyrin macrocycle into the related chlorin is of great synthetic significance. Can it be done by using the porphyrin macrocycle as a dienophile?

We have shown for the first time in 1997 that porphyrin macrocycles without vinyl substituents can react as dienophiles in the presence of reactive dienes which, in some cases, are generated *in situ*.<sup>22,26,27</sup> Usually chlorins are the main products obtained, but, depending on the physical-chemistry features of the starting porphyrin, other products such as bacteriochlorins or isobacteriochlorins can also be obtained. The initial studies in this area started with *meso*-tetrakis(phenyl)porphyrin (TPP) **5** and the diene (*ortho*-benzoquinodimethane) generated *in situ* by thermal extrusion of SO<sub>2</sub> from benzosulfone **6** (

Scheme 2). *meso*-Tetrakis(3-methoxyphenyl)porphyrin and *meso*-tetrakis(4-methoxyphenyl)porphyrin have also been used. The corresponding annulated chlorins like **7** have been the main isolated products. Starting with *meso*-tetrakis(pentafluorophenyl)porphyrin, not only the chlorin but also two stereoisomeric (*cis* and *trans*) bacteriochlorins **8a** and **8b** were isolated (

Figure 7).<sup>23</sup>



**Scheme 2.** [4+2] Cycloaddition of TPP with *o*-benzoquinodimethane.

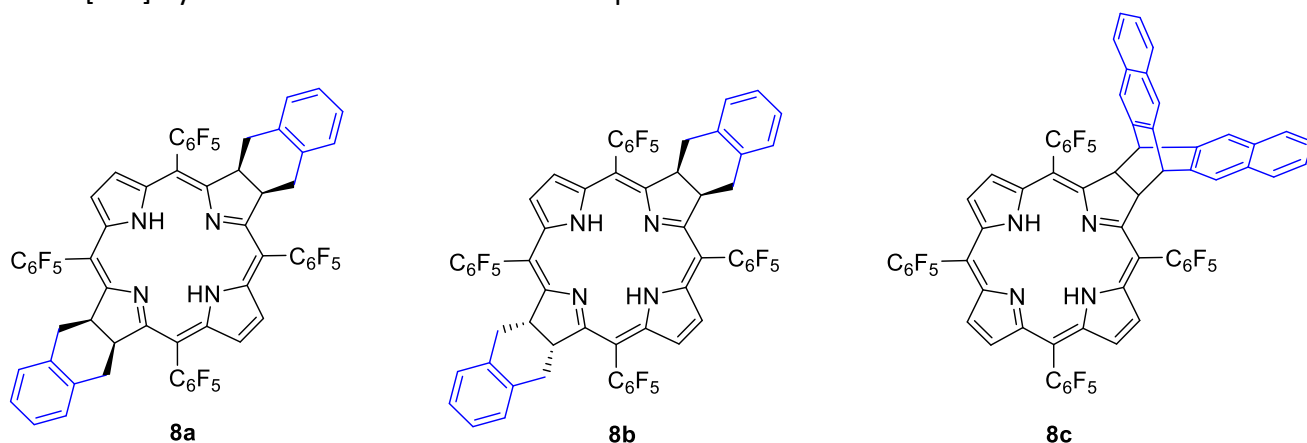


**Figure 7.** Structures of the two obtained stereoisomeric bacteriochlorins **8a** and **8b** and the barrelene-chlorin **8c**.

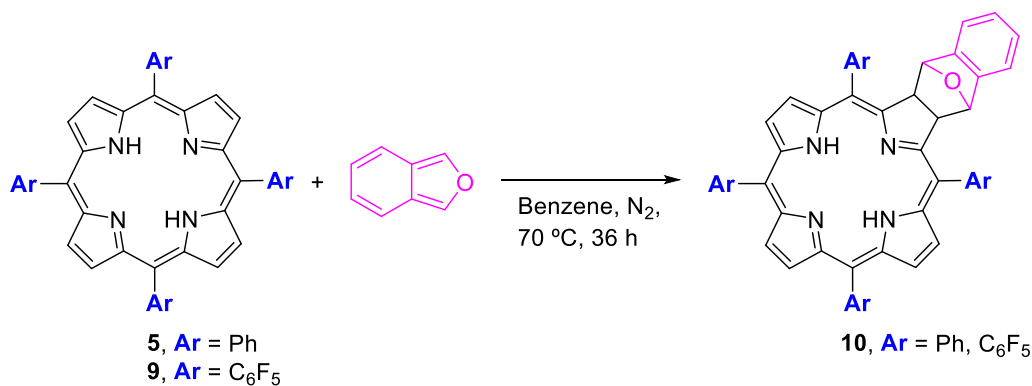
The method was extended to polyaromatic compounds considered to be stable dienes, such as pentacene and tetracene.<sup>27,28</sup> The former gave rise to a barrelene-chlorin by cycloaddition across the pentacene 6,13 positions (**8c**, Figure 7); the latter, under microwave irradiation, gave rise to two isomeric chlorin derivatives.

Herges *et al.*<sup>29</sup> have applied this synthetic procedure for the synthesis of chlorins, bacteriochlorins and isobacteriochlorins. Isobenzofuran (IBF) was used as the diene and *meso*-tetrakis(pentafluorophenyl)porphyrin (TPP) **5**, *meso*-tetrakis(pentafluorophenyl)porphyrin **9**, and their Ni(II) complexes, as the dienophiles. Interestingly, these [4+2] cycloadditions took place at 70 °C (

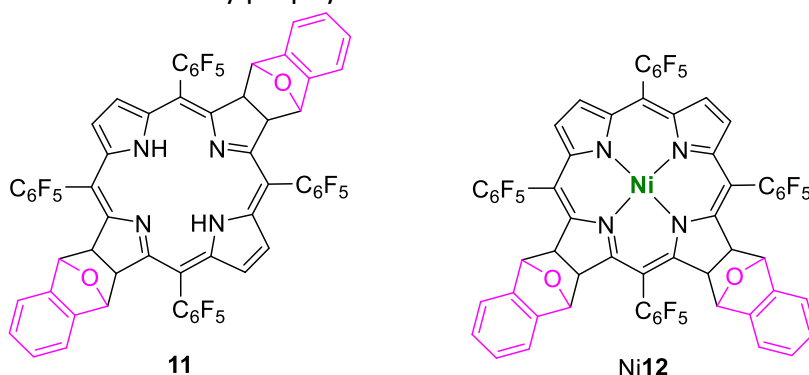
Scheme 3). Depending on the amount of IBF used, the reaction with *meso*-tetrakis(pentafluorophenyl)porphyrin free base **9** gave, as the main product, the chlorin **10** or the bacteriochlorin **11**; its Ni(II) complex gave the isobacteriochlorin Ni**12** as the main or the only product (

Figure 8). In the reaction with the free base **9**, the chlorin was the only product, while with the Ni(II) complex no product was isolated. Furthermore, the studied cycloadditions were claimed to be regio- and stereoselective.



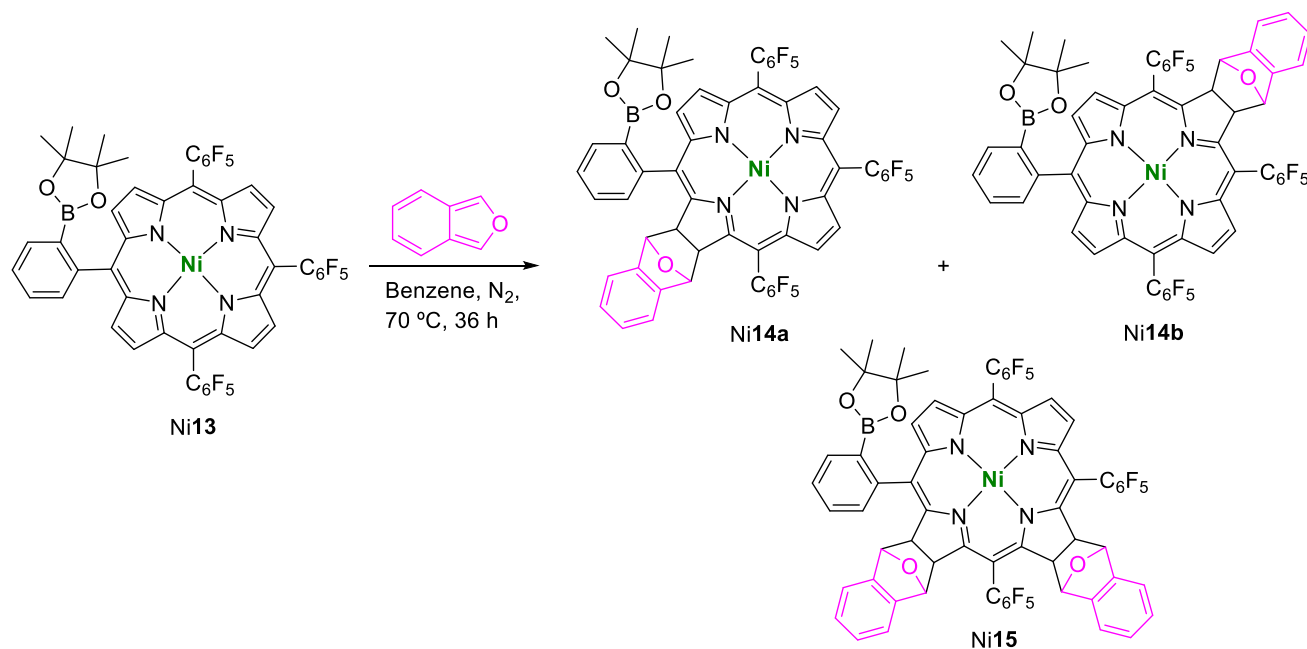


**Scheme 3.** Cycloaddition of *meso*-tetraarylporphyrins with IBF.



**Figure 8.** Structures of bacteriochlorin (**11**) and isobacteriochlorin (**Ni12**).

The same group used the [4+2] method for the synthesis of borylated Ni(II) chlorins (**Ni14a** and **Ni14b**) and Ni(II) isobacteriochlorins **Ni15** from IBF and **Ni13**, the Ni(II) complex of the corresponding borylated porphyrin (Scheme 4).<sup>30</sup> When the free-base borylated porphyrin was used, the isolated products were the free-base chlorins and the bacteriochlorin.



**Scheme 4.** [4+2] Cycloaddition of borylated porphyrin **Ni13** with IBF.

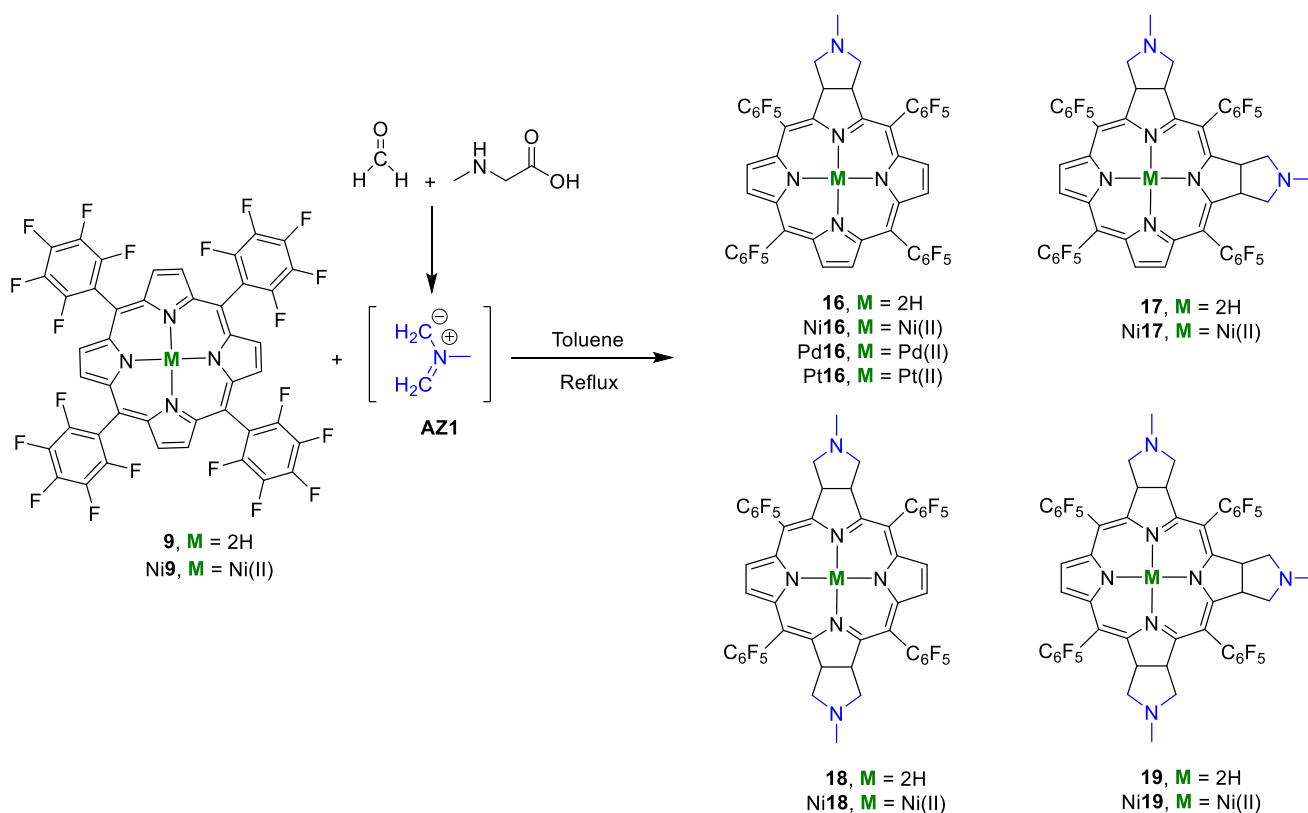
### 3. 1,3-Dipolar cycloadditions

#### 3.1. Reaction of porphyrins with azomethine ylides

The possibility of porphyrins acting as dipolarophiles in 1,3-dipolar cycloadditions with azomethine ylides was reported for the first time by Cavaleiro and co-workers in 1999.<sup>31,32</sup> The impact of this approach, to obtain high-value chlorins and other bis-adducts, is patent by the high number of scientific publications that appeared after the Cavaleiro's seminal work and by the applications of the prepared compounds in different fields namely as catalysts,<sup>33–35</sup> sensors, therapeutics for cancer, antimicrobial, antiviral or other biomedical applications.<sup>36</sup>

In these pioneering studies, the azomethine ylide **AZ1** was generated *in situ* from the reaction of paraformaldehyde and *N*-methylglycine (sarcosine) in refluxing toluene in the presence of TPP **5**, *meso*-tetrakis(2,6-dichlorophenyl)porphyrin and *meso*-tetrakis(pentafluorophenyl)porphyrin **9**. In general, as exemplified in

Scheme 5 for porphyrin **9**, the major products were the corresponding chlorin **16** and isobacteriochlorin **17**. Although the bis-addition is highly site-selective to afford the isobacteriochlorins **17**, the bacteriochlorin **18**, and the tris-adduct **19** could also be obtained under more forcing conditions.<sup>32,37</sup>



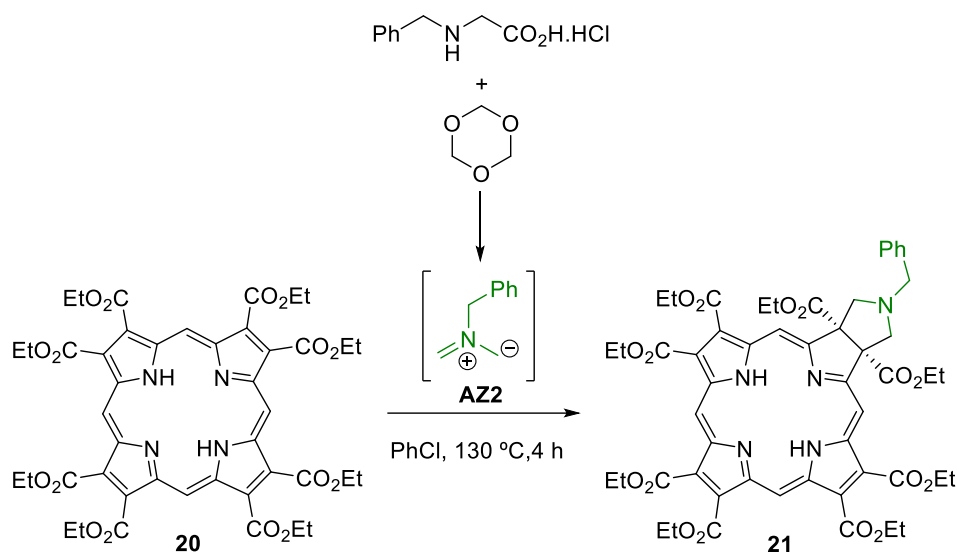
**Scheme 5.** 1,3-Dipolar cycloaddition of *meso*-tetrakis(pentafluorophenyl)porphyrin **9** and azomethine ylide **AZ1**.

In those earlier studies, the possibility to generate azomethine ylides using other amino acids (*e.g.* glycine, *L*-proline and *trans*-4-hydroxy-*L*-proline) or other aldehydes namely with sugar units, was also considered and *N*-

H pyrrolidine-fused chlorins or a series of *N*- and *C*-glycoconjugated pyrrolidine-fused chlorins were prepared.<sup>32,38</sup>

The extension of this approach to porphyrins of A<sub>3</sub>B type, bearing three pentafluorophenyl groups and one pyridyl unit at *meso*-positions, was also successful, affording the expected chlorins,<sup>39</sup> while in porphyrins with electron-withdrawing groups (*e.g.* alkyloxycarbonyl substituents) at vicinal  $\beta,\beta'$ -pyrrolic positions, the cycloaddition occurred preferentially at the activated double bond affording “locked chlorins”.<sup>40,41</sup>

A similar “locked chlorin” **21** was obtained from the reaction of  $\beta$ -octa(ethyloxycarbonyl)porphyrin **20** with azomethine ylide **AZ2** through a 1,3-dipolar cycloaddition (



**Scheme 6.** 1,3-Dipolar cycloaddition of  $\beta$ -octa(ethoxycarbonyl)porphyrin **20** with azomethine ylide **AZ2**.

The functionalization of  $\beta$ -octa(ethoxycarbonyl)porphyrin scaffolds through 1,3-dipolar additions with bulky azomethine ylides exhibits two main drawbacks compared with *meso*-tetraarylporphyrins. The first one is the difficulty to prepare the corresponding bacteriochlorin in appreciable amounts; the authors only observed the formation of the double-reduced derivative in very small amounts, even when the reaction was performed in the presence of large amounts of the 1,3-dipole precursors, leading to degradation of the reaction mixture. Under these conditions, the reaction of the Zn(II) complex of porphyrin **20** did not give rise to any reduced derivative, and only partial recovery of the starting material was possible. However, with the modification leading to chlorin **21** non-aggregation properties were demonstrated by the chlorin derivative; this feature, combined with the high fluorescence quantum yield and good singlet oxygen generation capability, makes chlorin **21** to be a good candidate for use in medicinal applications, such as a fluorescent marker and photosensitizer, opening the possibility for the compound to be exploited in theranostics.<sup>43</sup>

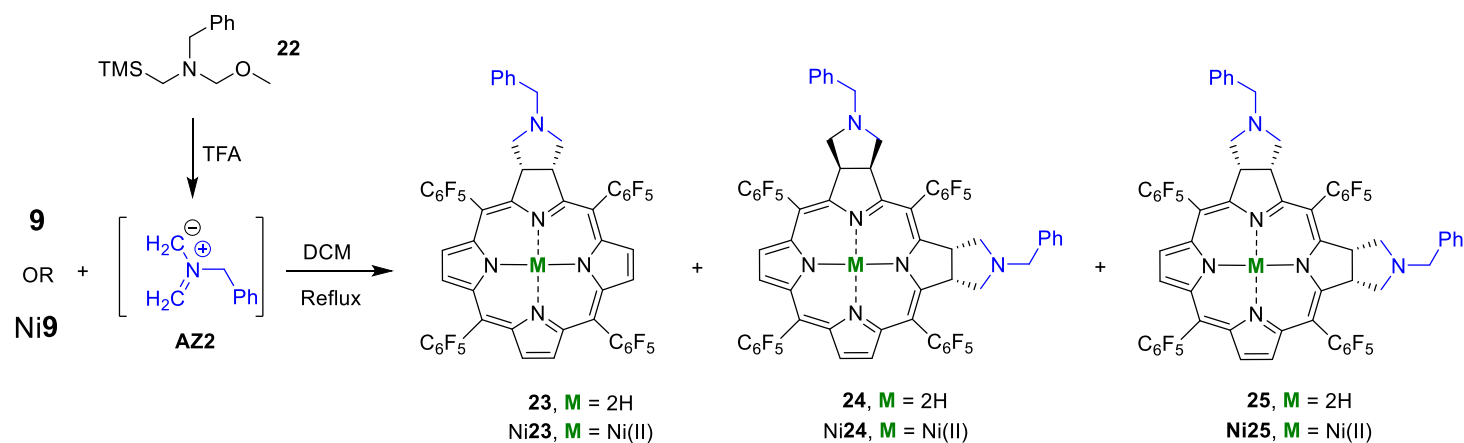
The selection of *meso*-tetrakis(pentafluorophenyl)porphyrin **9**, which contains four electron-withdrawing groups at *meso* positions, as starting material for the preparation of chlorins through 1,3-dipolar cycloadditions, is not unexpected considering its high reactivity towards azomethine ylides. Additionally, further functionalization of the C<sub>6</sub>F<sub>5</sub> units through nucleophilic substitution of the *para*-fluorine atoms<sup>9</sup> with a range of

nucleophiles allowed the expansion of the library of this type of chlorins with improved features for PDT and other applications. Also, the presence of fluorine atoms makes these compounds amenable as probes for *in vivo*  $^{19}\text{F}$  NMR localization studies. Moreover, the incorporation of metals in the inner core of the reduced adducts opened new perspectives in terms of their applications in different fields as previously mentioned. For instance, in the context of PDT applications, Obata *et al.*<sup>44</sup> selected chlorin **16** and the corresponding Pd(II) and Pt(II) complexes (Pd**16** and Pt**16**) to evaluate the impact of the heavy atom effect on their performance as photosensitizers in PDT. The presence of a heavy atom on the photosensitizer molecule generally facilitates intersystem crossing and, consequently, the population of the triplet manifold, improving the singlet oxygen ( $^1\text{O}_2$ ) quantum yield ( $\phi_\Delta$ ), which is a key species in the PDT mechanism of action. The results showed that the  $\phi_\Delta$  values increased in the following order: **16** (0.28) < Pd**16** (0.89) < Pt**16** (0.92) in  $\text{C}_6\text{D}_6$  and their photocytotoxicity towards HeLa cells (light dose of  $16\text{ J}\cdot\text{cm}^{-2}$  with  $\lambda > 500\text{ nm}$ ) increased in the same order (**16** < Pd**16** < Pt**16**) at a concentration of  $0.5\text{ }\mu\text{M}$ . The study also showed that, upon photoirradiation, chlorins **16**, Pd**16** and Pt**16**, at a concentration of  $5\text{ }\mu\text{M}$ , killed almost all cells, while the corresponding porphyrins showed no photocytotoxicity under the same conditions, possibly due to their poor light-absorbing properties.<sup>44</sup>

The nucleophilic substitution of the *para*-fluorine atoms was also particularly relevant to open new therapeutic perspectives for chlorin **16**, namely through the attachment of carboranyl groups,<sup>45</sup> sugar units,<sup>46–49</sup> amongst others. Considering the number of studies reported during the last decade, the relevance of the reaction of porphyrins with azomethine ylides is obvious.

In 2014, Oliveira *et al.*,<sup>50</sup> looking for azomethine ylides precursors to perform the cycloaddition reactions under milder conditions,<sup>51,52</sup> studied the reaction of **9**, and its nickel complex Ni**9**, with the dipole **AZ2** which was generated from precursor **22** with TFA in dichloromethane (

Scheme 7). This precursor was obtained from the reaction of benzylamine and (chloromethyl)trimethylsilane, followed by reaction with aqueous formaldehyde in methanol. The best results were obtained with the Ni(II) complex and depending on the number of equivalents of **22**, it was possible to obtain chlorin Ni**23** or the isobacteriochlorins Ni**24** and Ni**25**. It was also found that the free-bases (**23–25**) were easily obtained by demetallation in  $\text{CH}_2\text{Cl}_2/\text{H}_2\text{SO}_4$ .



**Scheme 7.** Chlorin and isobacteriochlorins isolated from the reaction of azomethine ylide **AZ2** with porphyrin **9** or its nickel(II) complex Ni**9**.

Under the context of biological applications, in 2014 Drain and co-workers<sup>53</sup> reported a comprehensive study concerning the photophysical/photochemical properties (fluorescence quantum yield, singlet state lifetime, triplet quantum yield, two-photon absorption and quantum yield of singlet oxygen formation) of porphyrin **9**,

and of the corresponding chlorin **16**, isobacteriochlorin **17** and bacteriochlorin **18**. Having in mind that glycosyl groups are able to target many cancer cell types because of their significantly increased number of glucose transporters and lectin-type receptors in the membrane, the authors extended the study to the corresponding non-hydrolysable thioglycosylated conjugates **26–29** (

Figure 9) obtained through the nucleophilic substitution of the *para*-fluorine atoms with the adequate sugar unit.

Following the photophysical features found for the compounds under study, the authors came to the following conclusion: that the isobacteriochlorins **17** and **28** have a sufficient two-photon absorption (2PA) and emission to obtain high-quality two-photon microscopy images. These results also suggest that **28** is a good candidate for simultaneous imaging and PDT using near-IR light. Because of the significantly stronger Q bands at 730 nm and high triplet quantum yield, the glycosylated bacteriochlorin **29** has good potential as a PDT agent under single-photon conditions. In addition, the glycosylated chlorin **27** has photophysical properties that may be used for both detection and ablation of cancer. The compounds were also found to be photostable under experimental conditions and both **26** and **27** showed a notable capacity to inhibit head and neck squamous carcinoma xenograft tumor model in mice under standard light conditions.

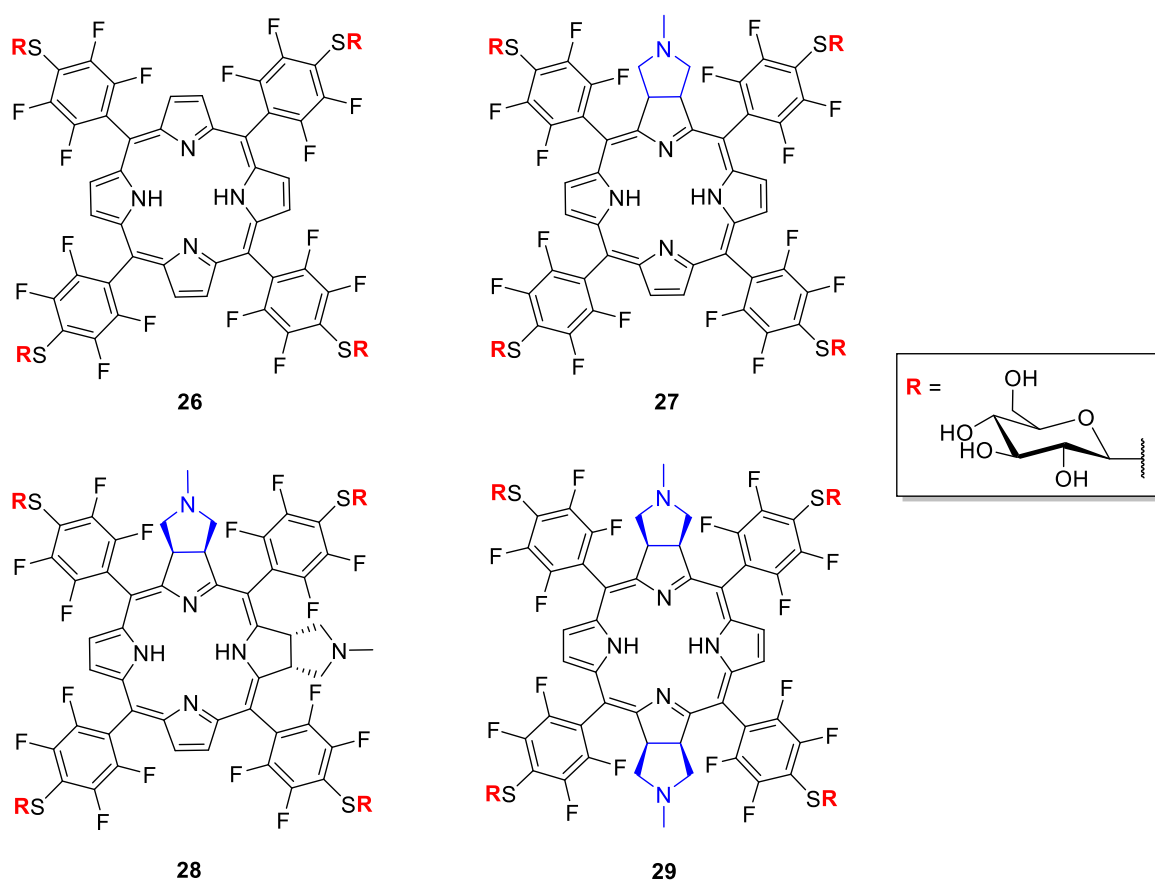


**Figure 9.** Structures of porphyrin (**26**) and of the corresponding chlorin (**27**), isobacteriochlorin (**28**) and bacteriochlorin (**29**) functionalized with thioglycosyl units.

In 2016, Narumi *et al.*, considering that a PS with good water solubility can avoid cutaneous phototoxicity due to their rapid clearance from the body,<sup>54</sup> reported the development of **32** bearing four maltotriose units (

Figure 10). The synthetic approach involved the reaction of chlorin **16** with the protected maltotriose **30** in the presence of diethylamine, followed by the deprotection reaction of the oligosaccharide moieties of **31** with sodium methoxide (

Figure 10). The authors mentioned an improvement in the water-solubility of the resulting oligosaccharide conjugate when compared with previously reported monosaccharide counterparts with glucose units<sup>46</sup> and a very high photodynamic activity towards HeLa cells (95% of killing at 3.0  $\mu\text{M}$ , irradiation conditions  $\lambda > 610\text{ nm}$  for 30 min) with a  $\text{IC}_{50}$  of approximately 1.3  $\mu\text{M}$  for the selected assay system. The higher efficacy of the chlorin **32**, when compared with the analogous porphyrin also synthesized, under identical irradiation conditions (reduction of cell viability to 35% at 5.0  $\mu\text{M}$ ) was also commented on. The high photodynamic activity of this water soluble chlorin, attributed to its efficiency to generate  $^1\text{O}_2$ , opens new perspectives for its use *in vivo* as an injectable PS.

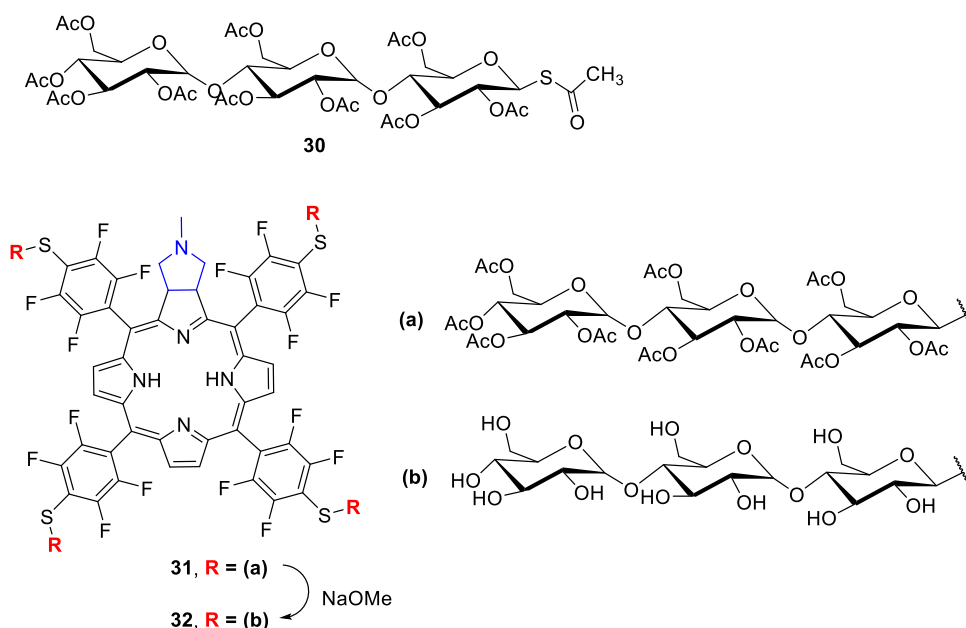


**Figure 10.** Structures of chlorins **31** and **32** functionalized with maltotriose units.

In the same period, and also under the context of biological applications, chlorin **16** was selected as scaffold in the rational design of the third-generation photosensitizer **34** bearing galactodendritic units (

Figure 11).<sup>55</sup> The synthetic approach also involved the nucleophilic substitution of the *para*-fluorine atoms of the *meso*-tetrakis(pentafluorophenyl)chlorin **16** by galactodendritic units, giving **33**, followed by the deprotection step of the sugar units, affording **34**. The effectiveness of PS **34** was evaluated towards UM-UC-3 and HT-1376 bladder cancer cells, and the promising results obtained were in line with its photochemical and photophysical properties (like the ability to generate singlet oxygen, to interact with the proteins galectin-1 and human serum albumin (HSA) and to its high absorption in the red region of the electromagnetic spectrum). The results revealed that a single dose of light irradiation is necessary to induce high cytotoxicity towards UM-UC-3 bladder cancer cells, while for HT-1376 bladder cancer cells resistant to therapy, the photodynamic efficacy is improved after a second light irradiation treatment. This enhanced phototoxicity in HT-1376 cancer cells was justified by considering the ability of **34** to accumulate in the mitochondria, mediated by glucose transporter 1 (GLUT1), in the period between single and repeated irradiation.

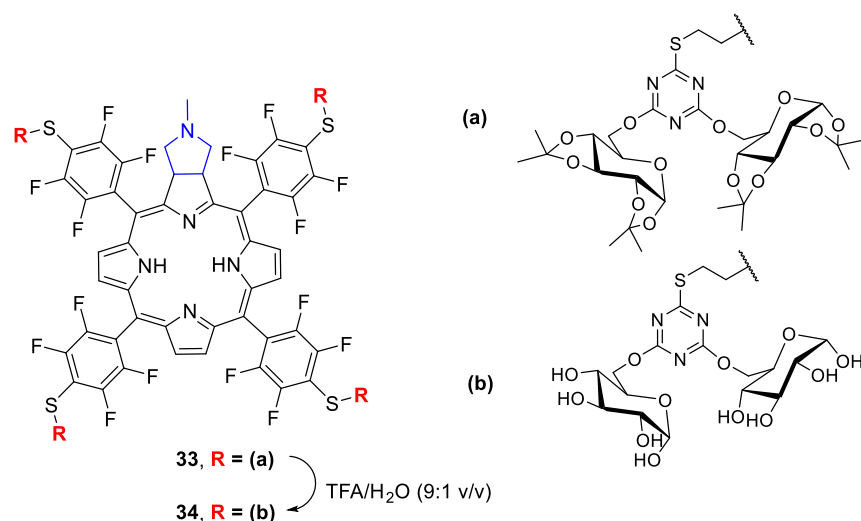
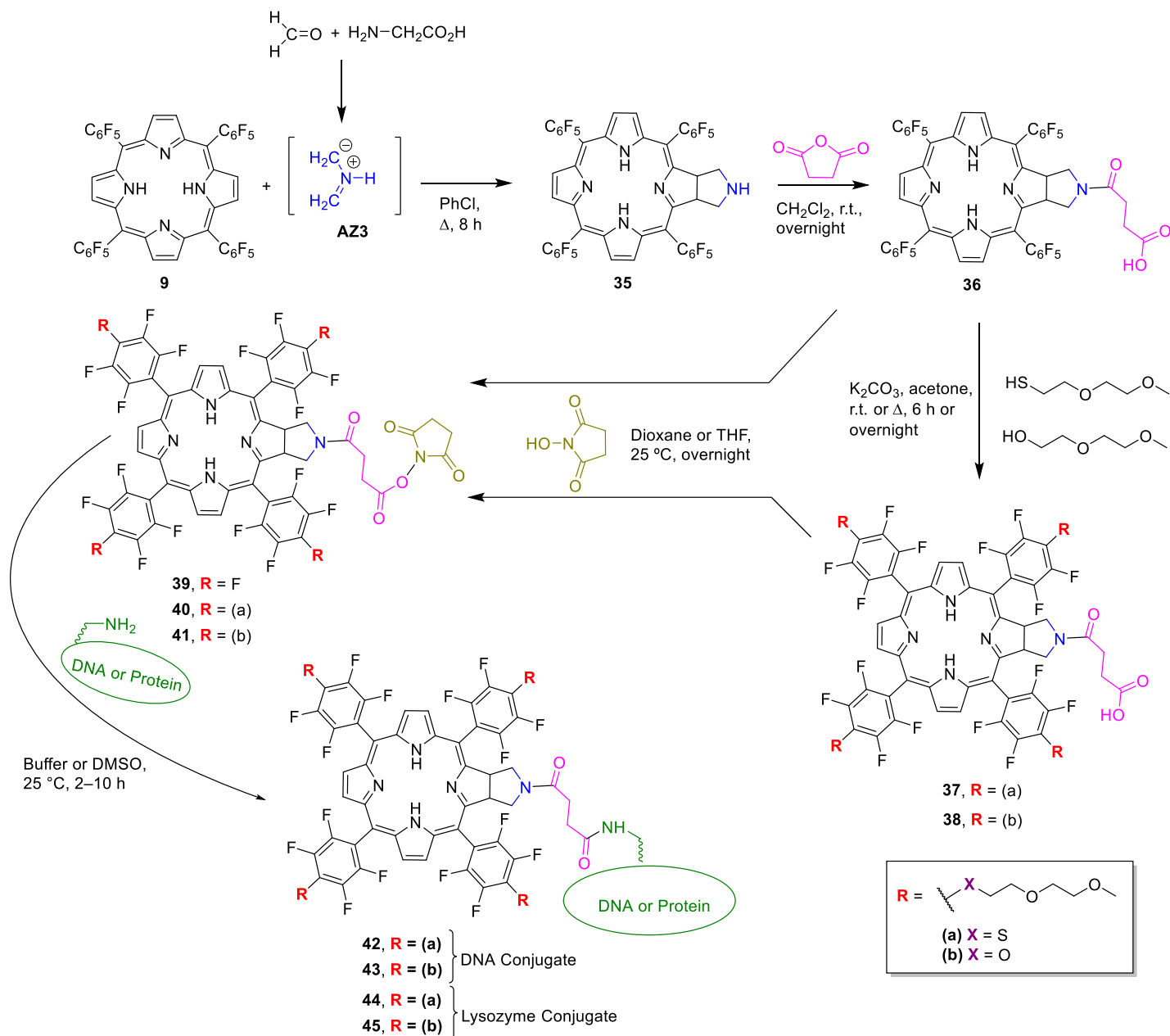


**Figure 11.** Structures of chlorins **33** and **34** functionalized with galactodendritic units.

In 2017, Drain and co-workers<sup>56</sup> selected the *NH* chlorin **35**, obtained from the reaction of **9** with paraformaldehyde and glycine (ylide **AZ3**), to obtain the chlorin derivative **36** and from this one the multifunctional chlorin platforms **37** and **38** appended with short polyethylene glycols [2-(2-methoxyethoxy)ethanol (O-PEG) and 2-(2-methoxyethoxy)ethanethiol (S-PEG) groups] and a carboxylate-linker (

Scheme 8). This acid linker was considered to allow a rapid conjugation of the chlorins to bio targeting motifs such as proteins and oligonucleotides. As a proof of concept, the conjugation of derivatives **40** and **41** to a primary amine tethered on the 5' end of a 14 nucleotide (nt) single-strand DNA and to the exposed lysine amino groups on the lysozyme enzyme was reported, affording respectively derivatives **42–45** after activation of the carboxylic functionality with *N*-hydroxysuccinimide. The possible uptake of the DNA–chlorin conjugate **43** by MDA-MB-231 breast cancer cells was evaluated and the results seemed to indicate that the aggregates observed at concentrations above 5 nM in/on the cells slowly disaggregate.



**Scheme 8.** Synthetic approach to chlorin–protein and chlorin–DNA conjugates.

Later, the authors revisited the synthetic approach previously reported by Cavaleiro and co-workers<sup>32</sup> to obtain the NH-chlorin **35** from paraformaldehyde and glycine (**AZ3**), and an improvement of its formation by using microwave heating was reported.<sup>57</sup> During this endeavor, besides the expected NH-pyrrolidine, two dimers, and the same *N*-methyl chlorin obtained from the sarcosine ylide reaction were isolated. A mechanism based on the formation of the divergent *N*-(hydroxymethyl)-*N*-methylenemethaniminium ylide was considered.

In 2020, an approach mediated by the divergent *N*-(hydroxymethyl)-*N*-methylenemethanimine ylide was extended to obtain chlorins **46** and **47** with amino and alkynyl linkers, thereby enabling other types of click chemistry for bioconjugation (



Figure 12).<sup>58</sup> In this work an optimized approach to obtain the NH pyrrolidine **35** from a dimeric chlorin precursor was reported. Also, synthetic access to Cu(II), Ni(II) and [<sup>64</sup>Cu] complexes Cu**48**, Ni**48** and [<sup>64</sup>Cu]**49**, obtained from the previously reported chlorin **36** bearing the carboxyl functionality, was considered and new perspectives for their use in fluorescent imaging and positron emission tomography (PET) became available. This assumption was confirmed<sup>59</sup> when the conjugates obtained from the free-base chlorin **36** and [<sup>64</sup>Cu]chlorin **49** with the peptide Hsp1a isolated from the venom of the Peruvian tarantula *Homeomma spec.*, were demonstrated to be excellent reporters to localize peripheral nerves by fluorescence and Cerenkov luminescence imaging.

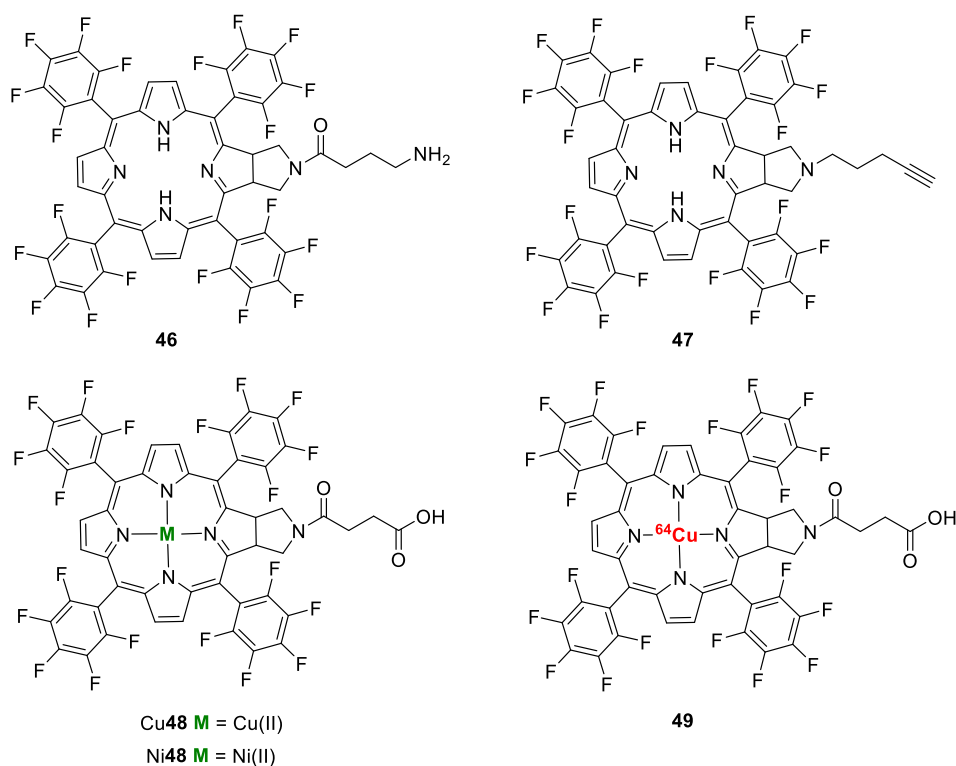
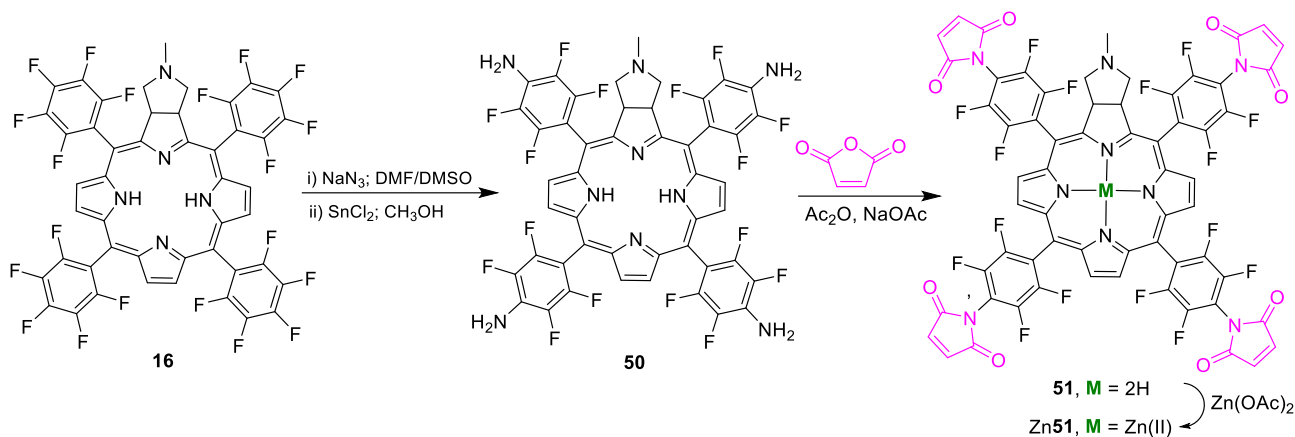


**Figure 12.** Free-bases and metal complexes of chlorins with amino, alkyne and carboxyl functionalities (**46-49**).

In 2019, Ol'shevskaya *et al.*<sup>60</sup> selected chlorin **16** as a scaffold to obtain the maleimide-functionalized chlorin **51** and its Zn(II) complex Zn**51** (

Scheme 9). This approach considered the substitution of the *para* fluorine atoms of **16** by azide ions, followed by its reduction to chlorin **50**. This chlorin was then converted into chlorin **51** by reaction with maleic anhydride. Although no biological activity has been reported yet, the authors commented that the presence of four maleimide groups in these chlorin derivatives could potentially improve their binding to proteins in living systems and consequently their biological activities.



**Scheme 9.** Synthetic approach to prepare maleimide-functionalized chlorins **51** and **Zn51**.

Considering that photodynamic therapy (PDT) can be an effective modality to treat several types of skin cancers, namely the most aggressive ones like melanoma, Castro *et al.*<sup>61</sup> decided to revisit the reaction of 5,10,15-tris(pentafluorophenyl)-20-(4-pyridyl)porphyrin **52** with the azomethine ylide **AZ1** and to evaluate the photodynamic action of the resulting chlorin **53** and isobacteriochlorin **54** (

Figure **13**) towards the melanotic cell line (B16F10 cells). For comparison, the studies were also extended to the starting porphyrin **52**. The best PDT effect was obtained with chlorin **53** under red LED light irradiation ( $\lambda = 660 \pm 20$  nm, light dose of  $5.4 \text{ J} \cdot \text{cm}^{-2}$ ) with cell death varying from 22.3% at a concentration of  $0.39 \mu\text{M}$  to 83.3% and 94.8% for concentrations of 6.2 and  $12.5 \mu\text{M}$  respectively. Under these irradiation conditions, **52** did not show any cytotoxicity while **54** showed only appreciable photocytotoxicity (72%) at concentrations higher than  $12.5 \mu\text{M}$ . From the internalization studies, it was suggested that the subcellular localization of **53** and **54** mainly occurs in the mitochondria due to apoptosis being the main death pathway. Also, the ability of **53** to generate peroxynitrite ( $\text{OONO}^-$ ) under irradiation, prompted the authors to hypothesize that its high photocytotoxicity could be due to a synergistic effect involving the production of singlet oxygen and  $\text{OONO}^-$ .

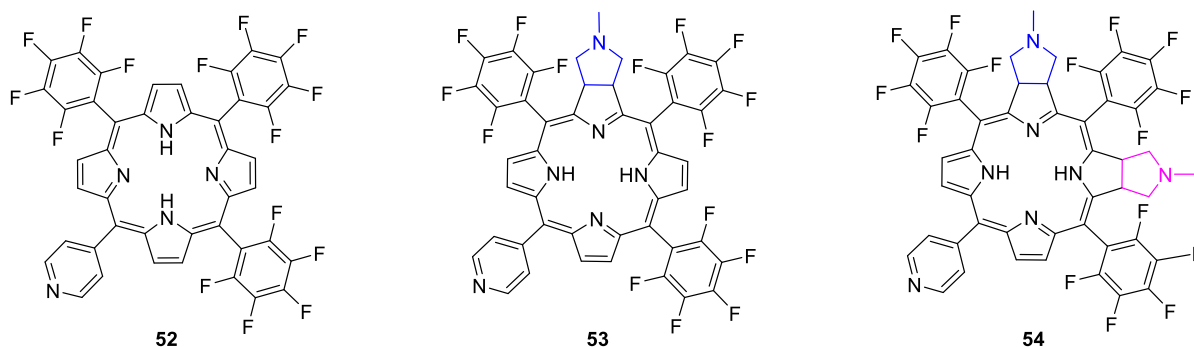


**Figure 13.** Structures of chlorin (**53**) and isobacteriochlorin (**54**) obtained from 5,10,15-tris(pentafluorophenyl)-20-(4-pyridyl)porphyrin (**52**).

Considering the recognized attractiveness of reduced-based PSs in cancer PDT, Mesquita *et al.*<sup>62</sup> reported in 2021 the efficacy of the hydrophobic fluorinated porphyrin **9**, chlorin **16** and isobacteriochlorin **17** (

Scheme 5), which were tested after being encapsulated in poly(vinylpyrrolidone) (PVP) micelles towards prostate cancer. The effectiveness of the nanoformulations obtained, namely **9@PVP**, **16@PVP** and **17@PVP** as PS agents, was evaluated *in vitro* towards a PC-3 cell line and the results revealed that at concentrations of 20  $\mu\text{M}$ , **16@PVP** and **17@PVP** were able to induce 53.1% and 87.9% of cell death respectively, after 4 h of incubation followed by 10 min of irradiation with red light (622 nm; irradiance of  $17.6 \text{ mW}\cdot\text{cm}^{-2}$ ). The studies also confirmed the involvement of a caspase-dependent pathway in the apoptotic response, following the PDT treatment mediated by **16@PVP** and **17@PVP**. It was commented that the impressive emission properties of **17**, combined with its high therapeutic action, open new perspectives for this formulation to be used as a theranostic agent.<sup>62</sup>

A recent study also showed that the pyrrolidine-fused chlorin of 5,15-bis(4-methyloxycarbonylphenyl)-10,20-bis-(pentafluorophenyl)porphyrin, incorporated into a metal-organic framework (MOF) functionalized with maltotriose, couldn't efficiently target cancer cells with preferential uptake into pancreatic and breast cancer cell lines.<sup>63</sup>

The use of chlorins and isobacteriochlorins obtained from the reaction of porphyrins and ylides as PSs in the photoinactivation of microorganisms was also considered in different studies. In 2012, Costa *et al.*,<sup>64</sup> reported the synthesis and the photodynamic action of the pentacationic chlorin **55** (

Figure 14) towards two antibiotic-resistant bacterial strains, *Staphylococcus aureus* and *Pseudomonas aeruginosa*. The synthetic approach involved in the first step the reaction of chlorin **16** with 4-mercaptopyridine, followed by alkylation of the neutral thiopyridylchlorin derivative with iodomethane. The antimicrobial photodynamic therapy (aPDT) treatments were performed with white light (400–800 nm) and red light (530–800 nm). The results were compared with the ones obtained with the cationic analog porphyrin and also with the well-known *meso*-tetrakis(1-methylpyridinium-4-yl)porphyrin tetra-iodide (TMPyP). These showed that chlorin **55** was the most effective PS for both antibiotic-resistant strains; for the Gram-positive bacterium *S. aureus* a reduction of 7.0 log units was observed after 5–10 min of irradiation, at a concentration of 0.5  $\mu\text{M}$ , whereas for the Gram-negative *P. aeruginosa*, a similar photoinactivation occurred at 10  $\mu\text{M}$  after 30 min of irradiation.

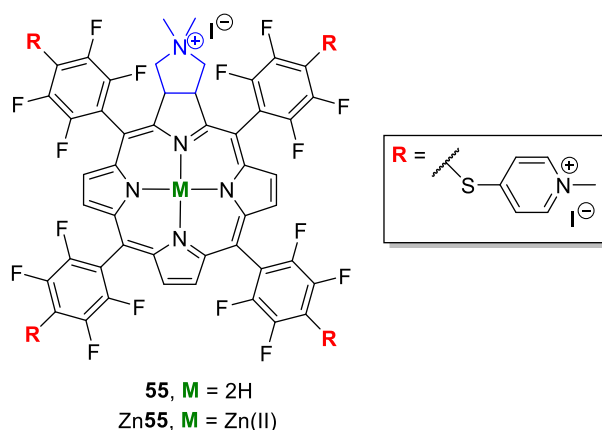


**Figure 14.** Structures of the pentacationic chlorin (**55**) and of the corresponding zinc(II) complex (**Zn55**) functionalized with (1-methylpyridinium-4-yl)sulfanyl moieties.

In 2014, Mesquita *et al.*<sup>65</sup> evaluated the efficacy of the cationic chlorin **56** and the isobacteriochlorin **57** (

Figure 15) in the photodynamic inactivation of bioluminescent *Escherichia coli* (*E. coli*). These cationic derivatives were obtained by alkylation of the corresponding neutral derivatives **16** and **17** and the biological results showed that there is a direct relationship between the inactivation efficiency and the increasing number of charges on the molecules. The aPDT treatment in the presence of the dicationic isobacteriochlorin reached the limit of detection (6.1 log reduction) after a light dose of  $36 \text{ J} \cdot \text{cm}^{-2}$  at  $20 \mu\text{M}$ . For the neutral compounds and the cationic chlorin, non-significant inactivation was detected.

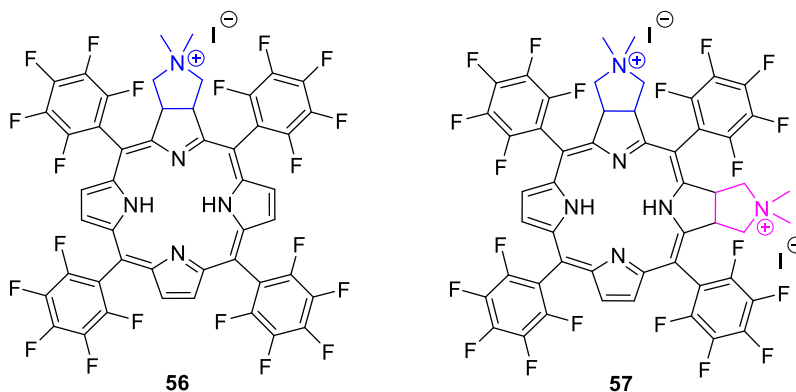


**Figure 15.** Structures of the cationic *meso*-tetrakis(pentafluorophenyl)chlorin (**56**) and isobacteriochlorin (**57**).

Soon afterwards, the same group found that the immobilization of the neutral chlorin **16** in 3-bromopropyl-functionalized silica and also in Merrifield resin-based materials provided promising photoactive materials towards *E. coli* (inactivation rates of *ca* 3.0 log at an irradiance of  $4.0 \text{ mW} \cdot \text{cm}^{-2}$ ) and that this bacterial reduction was maintained constant for at least three successive cycles of the aPDT treatment.<sup>66</sup>

In 2019, Calmeiro *et al.*<sup>67</sup> reported a similar methodology to the one reported in 2012 to obtain the free-base and the zinc(II) complex of the pyridinium chlorin derivatives **58** and Zn**58** (

Figure 16) and evaluated their efficacy to inactivate bioluminescent *E. coli*. The aPDT studies were also extended to the Zn(II) complex of the previously reported pentacationic chlorin Zn**55** (

Figure 14), which showed the best performance.

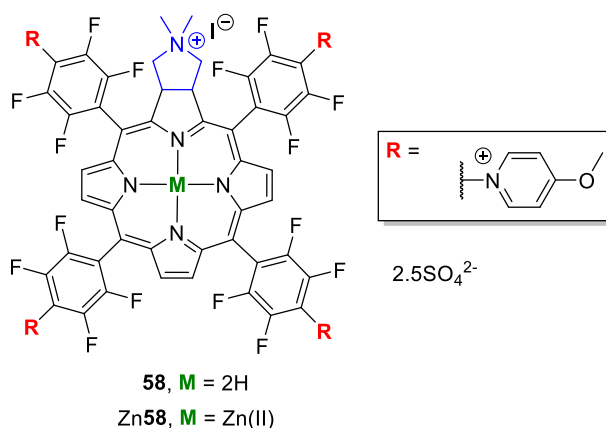


**Figure 16.** Pentacationic chlorin (**58**) and the zinc complex (Zn**58**) functionalized with 4-methoxy-1-pyridinium units.

In 2021, Lourenço *et al.*<sup>68</sup> also selected chlorin **16** to prepare the cationic PS chlorin **60** bearing 4-(1*H*-pyrazol-3-yl)pyridinium groups and their aPDT efficiency was investigated against planktonic and biofilm forms of the Gram-negative bacterium *E. coli* (

Figure 17). For comparison, the authors also synthesized the cationic porphyrin analog **59**. Although porphyrin **59** exhibited a higher antimicrobial efficiency against the planktonic cells of *E. coli*, chlorin **60** showed to be more efficient towards biofilms. This photodynamic efficiency can be related to the higher levels of  $^1\text{O}_2$  produced by **59**, as well as with the higher absorption in the red region exhibited by **60**.

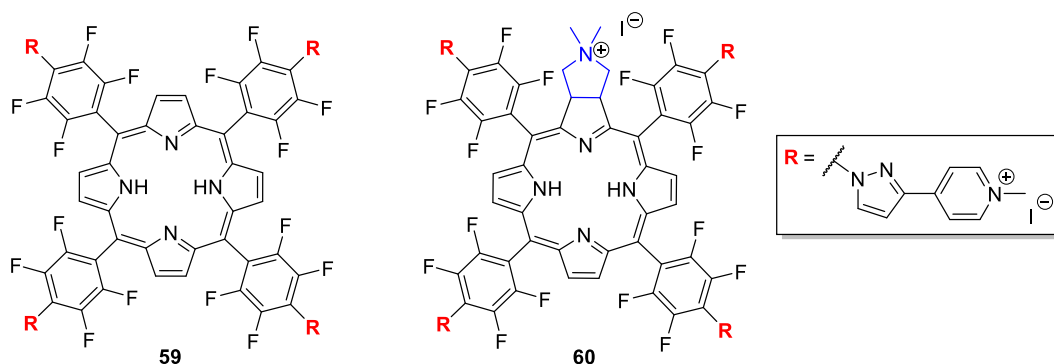


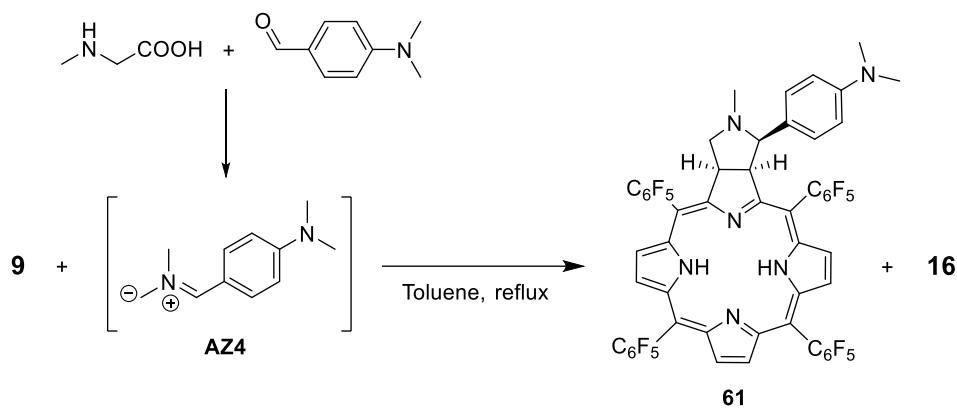
**Figure 17.** Cationic porphyrin (**59**) and chlorin (**60**) bearing 4-(1*H*-pyrazol-3-yl)pyridinium groups.

In 2018, the *meso*-tetrakis(pentafluorophenyl)porphyrin **9** was used by Durantini *et al.*<sup>69</sup> to prepare the pyrrolidine-fused chlorin **61** bearing a 4-(dimethylamino)phenyl residue. In this approach, the azomethine ylide **AZ4** was obtained from 4-(dimethylamino)benzaldehyde and *N*-methylglycine (

Scheme 10). However, due to the Strecker degradation of *N*-methylglycine to formaldehyde, **AZ1** was also formed and chlorin **16** was isolated as a side product (28%). The photophysical properties of the new compound have been investigated and it was found that **61** is a fluorescence quencher; this is presumably due to the 4-(dimethylamino)phenyl substituent appended at the macrocycle. In addition, for the same compound, the triplet excited state was not detected under laser flash photolysis studies and as consequence, no singlet oxygen generation was detected by time-resolved phosphorescence detection.

Nevertheless, the authors found a different outcome when **61** was submitted to an acidic medium – under these conditions the protonation of the amino group was attained, promoting the formation of singlet and triplet states that opened the way to photophysical channels leading to fluorescence emission and singlet oxygen generation, respectively. This pH switch prompted the authors to investigate the photodynamic effect of **61** towards bacteria in acidic medium and the results showed a highly efficient eradication of *E. coli*.

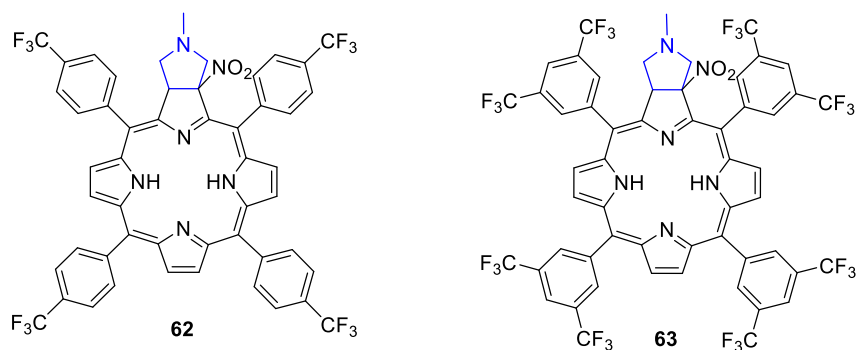
The fact that **61** can behave as an on/off molecular switch for the generation of singlet oxygen ( $^1\text{O}_2$ ), i.e. by being activated in acidic media and deactivated in neutral media, can be an advantage for the eradication of bacteria in the stomach which has an acidic environment.



**Scheme 10.** Synthesis of 4-(dimethylamino)phenyl-pyrrolidine-fused chlorin **61**.

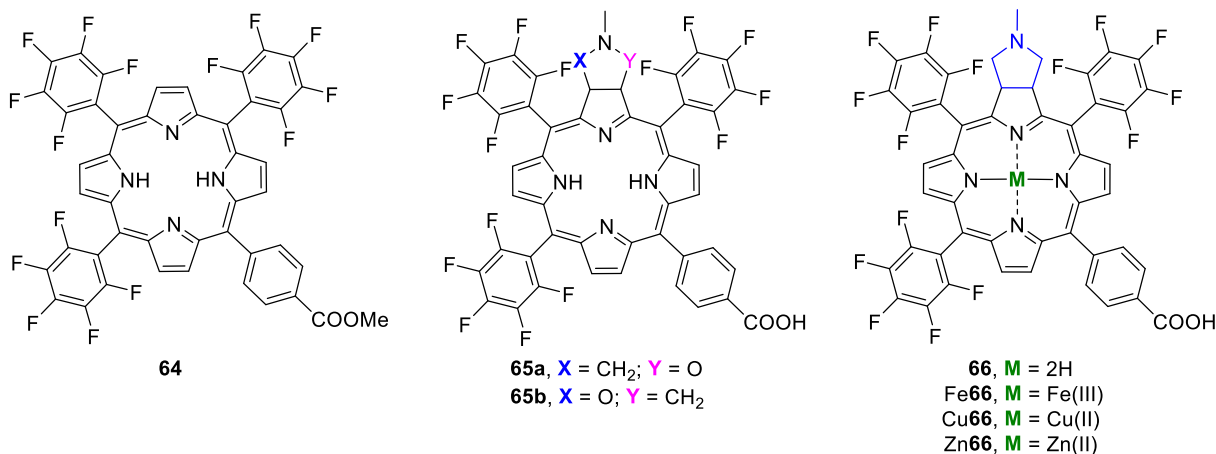
Sobota *et al.* selected the ylide **AZ1** to prepare chlorins **62** and **63** (

Figure **18**) via 1,3-dipolar cycloaddition from 2-nitroporphyrins bearing 4-(trifluoromethyl)phenyl or 3,5-bis(trifluoromethyl)phenyl substituents at *meso* positions.<sup>70</sup> After confirming the efficacy of both chlorins to generate singlet oxygen, their antimicrobial photodynamic action was evaluated after being incorporated in lipid vesicles. The best outcomes were observed with chlorin **63** with log reduction of 4.84 for *Enterococcus faecalis* and 4.09 for *Staphylococcus aureus* at 1  $\mu$ M; for *E. coli*, a reduction of 2.23 was only observed at 100  $\mu$ M. No activity was found against the fungi *Candida albicans* and *Trichophyton mentagrophytes*. In a previous work, detailed structural analysis of the *meso*-aryl rings motion in related unsymmetrical pyrrolidine-fused chlorins, including **62** and **63**, using NMR, UV spectroscopy and DFT theoretical calculations were reported.<sup>71</sup>



**Figure 18.** Structures of chlorins **62** and **63** obtained from the corresponding 2-nitroporphyrins.

In 2018, Silva *et al.*<sup>72</sup> used the reaction of the azomethine ylide **AZ1** with 5-(4-methoxycarbonylphenyl)-10,15,20-tris(pentafluorophenyl)porphyrin **64** to obtain the corresponding pyrrolidine-fused chlorin derivative **66** after hydrolysis of the ester group (Figure 19). A microwave irradiation protocol, using acetonitrile as solvent, was applied to obtain a series of metal complexes [Fe(III), Cu(II) and Zn(II)] from **64** and also the pyrrolidine-fused chlorin metal complexes from **66** (Fe**66**, Cu**66**, Zn**66**). The authors commented that the extension of this approach to *N*-methyl nitron, to afford isoxazolidine-fused chlorins **65**, provided lower yields and selectivity's (when compared with azomethine ylide as 1,3-dipole) with the disadvantage of a retro-cycloaddition reaction occurring to the isoxazolidine-fused chlorins during the acidic hydrolysis of the ester group.



**Figure 19.** 5-(4-Methoxycarbonylphenyl)-10,15,20-tris(pentafluorophenyl)porphyrin (**64**), isoxazolidine-fused chlorins (**65a,b**) and the pyrrolidine-fused chlorin derivatives (**66** and Fe, Cu, Zn complexes).

In 2021, the same group,<sup>73</sup> reported the extension of the protocol to obtain the *N*-methylpyrrolidine-fused *meso*-tetrakis(4-carboxyphenyl)chlorin **68**, from the symmetric *meso*-tetrakis(4-methoxycarbonylphenyl)-porphyrin **67** (

Figure 20). The incorporation of this chlorin into a nanostructured porous  $TiO_2$  matrix afforded a new material with high sensing efficiency able to detect the explosive triacetone triperoxide in the gas phase; this explosive is considered to be even more dangerous than the powerful nitroaromatics due to its extreme sensitivity to detonation upon impact, heating, or friction.

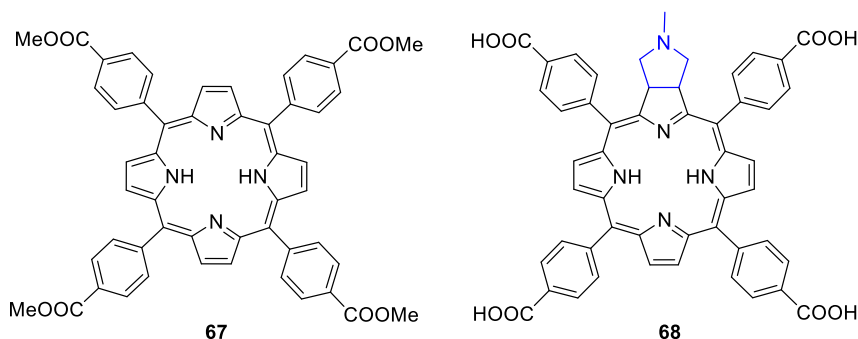


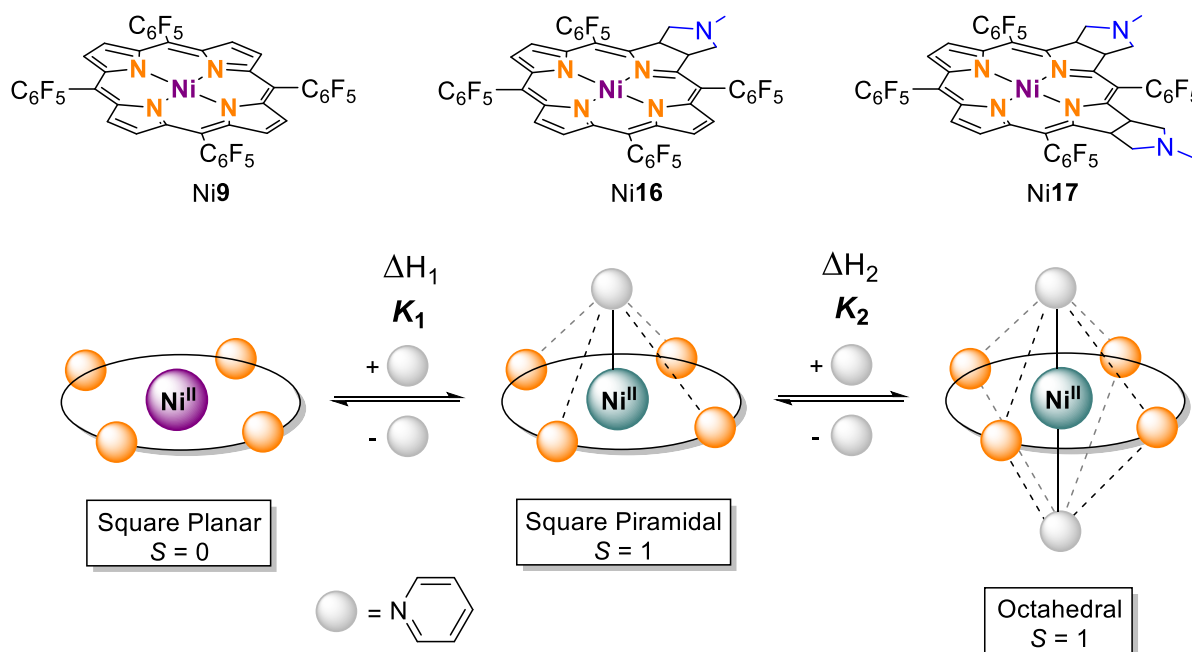
**Figure 20.** Structure of chlorin **68** obtained from 1,3-dipolar cycloaddition of **AZ1** with porphyrin **67** followed by hydrolysis of methyl ester units.

Herges *et al.*<sup>74</sup> reported that the square-planar chlorin and isobacteriochlorin Ni(II) complexes (**Ni16** and **Ni17**), and also the starting porphyrin **Ni9**, accomplish the preconditions for the design of efficient spin-switching systems (from  $S = 0$  to  $S = 1$ ); that is due to their ability to coordinate with axial ligands, thus affording the required square-pyramidal and octahedral complexes (Scheme 11).

The capability of the Ni(II) complexes **Ni16** and **Ni17** to act as spin-state switches (in the presence of pyridine the metal spin-state changes and the Ni(II) is able to axially coordinate pyridine molecules) was scrutinized by UV-vis spectroscopy and NMR titration experiments using pyridine as ligand. The results showed that the association constants  $K_1$  and  $K_2$  (determined by NMR spectroscopic titration) increase in the following order: porphyrin (**Ni9**) < chlorin (**Ni16**) < isobacteriochlorin (**Ni17**). With these findings it could be concluded that the



Ni(II) complexes **Ni16** and **Ni17** are good platforms for the coordination-induced spin-state switching (CISSS) and are potential candidates to be used as contrast agents in the field of medical imaging and interventional radiology.



**Scheme 11.** Coordination of **Ni9**, **Ni16** and **Ni17** with pyridine affording the corresponding nickel(II) complexes with square-pyramidal and octahedral geometries, with constants ( $K_1$  and  $K_2$ ) and formation enthalpies ( $\Delta H_1$  and  $\Delta H_2$ ).

Under the context of molecular spin switches' applications, Ikeue *et al.*<sup>75</sup> extended the method of Herges and prepared the stable diamagnetic ( $S = 0$ ) Ni(II) complex of pyrrolidine-fused pyrrocorphin **Ni19** (see

Scheme 5). The free-base of this hexahydroporphyrin was previously reported by Cavaleiro and co-workers<sup>31</sup> and contrary to other pyrrocorphins it demonstrated to be less air sensitive.

The impact of the ligand in electronic features of the Ni(II) complex **Ni19** was also evaluated in the presence of pyridine. The addition of an excess of pyridine to **Ni19** in toluene solution yielded first the mono-pyridine five-coordinate complex and then the *bis*-pyridine six-coordinate paramagnetic complex ( $S = 1$ ). These compounds were characterized by employing several techniques as UV-Vis and <sup>1</sup>NMR spectroscopies, cyclic voltammetry, X-ray analysis and DFT calculations.<sup>75</sup>

The comparison of the binding constants obtained for the Ni(II) pyrrocorphin (**Ni19**) with the ones reported by Herges *et al.*<sup>74</sup> for the Ni(II) complexes of the corresponding porphyrin (**Ni9**), chlorin (**Ni16**), and isobacteriochlorin (**Ni17**) confirmed that the highest reduction of the porphyrin core is associated with a better performance in the desired coordination-induced spin-state switching (**Ni9** < **Ni16** < **Ni17** < **Ni19**).

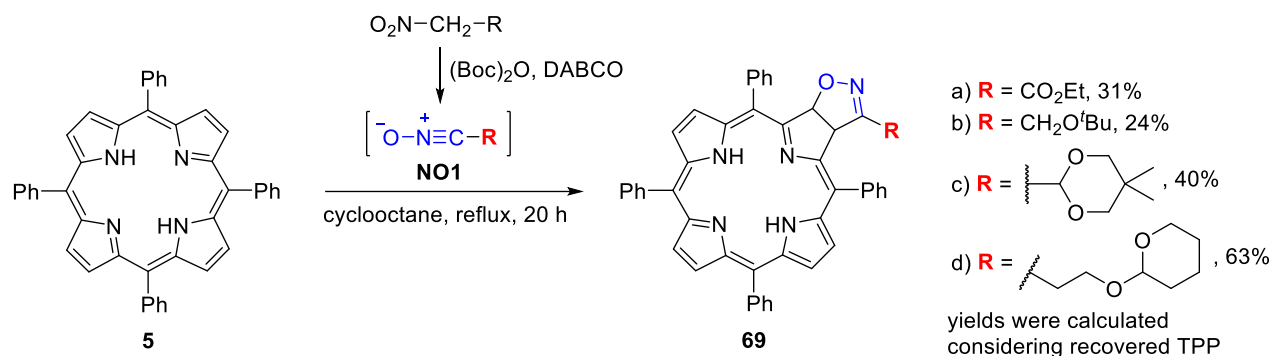
### 3.2 Reaction of porphyrins with nitrile oxides

Ostrowski *et al.*<sup>76</sup> reported that the reaction of TPP with alkyl nitrile oxides **NO1** afforded isoxazoline-fused chlorins **69** (

Scheme 12). Nitrile oxides **NO1** were generated *in situ* from unfunctionalized or functionalized nitroalkanes and a dehydrating agent (PhNCO or (Boc)<sub>2</sub>O) in the presence of an organic base (NEt<sub>3</sub> or DABCO). The yields



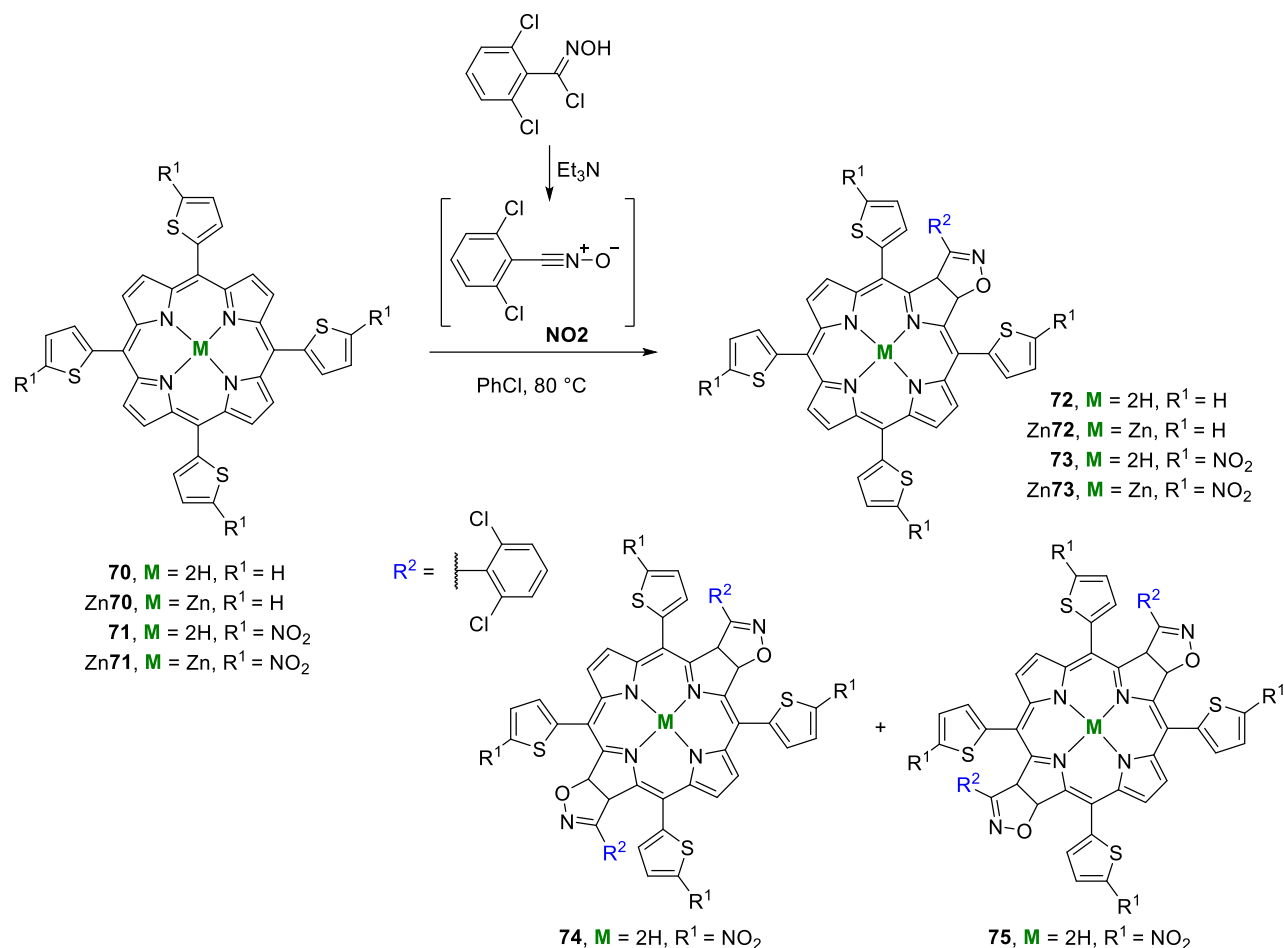
were low to moderate (most of the starting TPP was recovered) and best results were obtained using functionalized nitroalkanes. Chlorins **69a–d** were isolated in 24–63% yield considering the recovered TPP.



**Scheme 12.** Isoxazoline-fused chlorins **69** synthesized by reaction of TPP **5** and nitrile oxides.

The reaction of *meso*-tetra-2-thienylporphyrin (**70**) and *meso*-tetrakis(5-nitro-2-thienyl)porphyrin (**71**), both as free-bases and Zn(II) complexes, with 2,6-dichlorobenzonitrile oxide under various experimental conditions (

Scheme **13**), was studied by Oliveira *et al.*<sup>77</sup> The obtained products were the new chlorin derivatives **72**, **73** and their Zn(II) complexes Zn**72** and Zn**73**. The results showed that in these reactions the free-bases **70** and **71** were better dipolarophiles than the corresponding Zn(II) complexes and confirmed that the nitro derivative **71** was more reactive than **70**, affording the two regioisomeric bisadducts **74** and **75**, while no bisadducts were formed from **70**.



**Scheme 13.** 1,3-Dipolar cycloaddition of (2-thienyl)porphyrins with 2,6-dichlorobenzonitrile oxide.

Feng *et al.*<sup>78</sup> reported the reaction of an AB<sub>3</sub>-type porphyrin with 2,6-dichlorobenzonitrile oxide and obtained a mixture of the four expected site- and regio-isomeric monoadducts (illustrated with structure **76a**) and the bacteriochlorin bisadduct **77** (

Figure **21**). The five products (each obtained in *ca.* 10% yield) were separated by column chromatography on silica gel. Metalation and alkaline hydrolysis of the ester group of the four monoadducts afforded the corresponding Ni(II) porphyrin carboxylic acids (illustrated with structure **76b**) which were then used in dye-sensitized solar cells. The highest conversion efficiency of 3.65% with a short circuit photocurrent density of 8.55 mA/cm<sup>2</sup>, an open-circuit voltage of 610 mV, and a fill factor of 0.70 was obtained for one of the isomers.

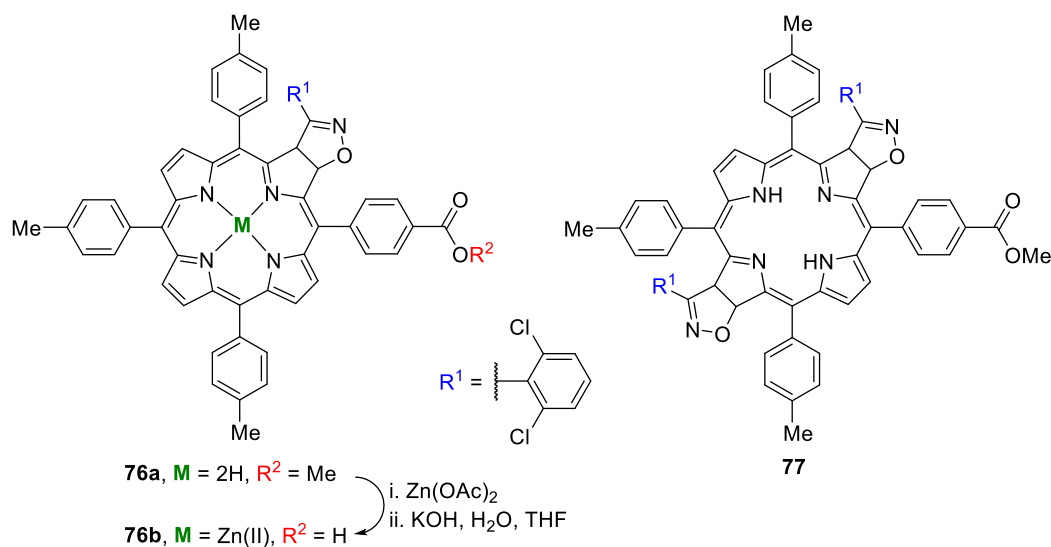
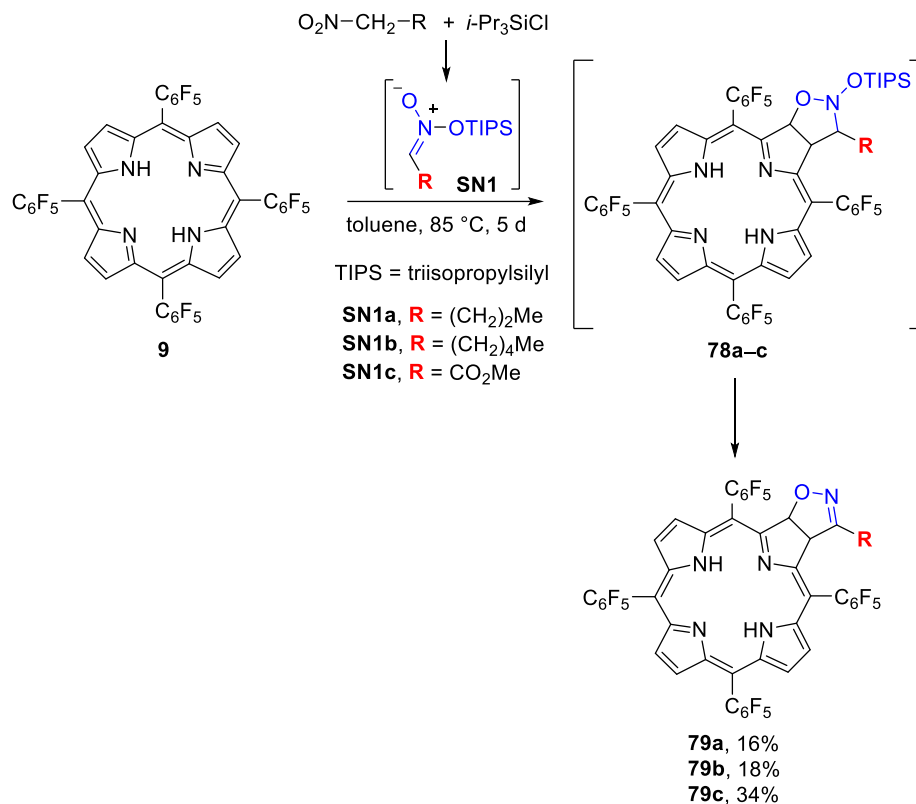


**Figure 21.** Structures of chlorins **76a,b** and bacteriochlorin **77**.

### 3.3. Reaction of porphyrins with silyl nitronates

Isoxazoline-fused chlorins of type **79** are typically prepared from the 1,3-dipolar cycloaddition of porphyrins with nitrile oxides, as shown in the previous section. However, considering that the yields of those reactions are frequently low, Senge *et al.*<sup>79</sup> studied an alternative strategy to obtain isoxazoline-fused chlorins from porphyrins and silyl nitronates (SN). Silyl nitronates are 1,3-dipoles that behave as synthetic equivalents of nitrile oxides. As shown in

Scheme **14**, *meso*-tetrakis(pentafluorophenyl)porphyrin (**9**) reacted with silyl nitronates **SN1a–c** (generated from the corresponding aliphatic nitro compounds and triisopropylsilyl chloride) to give, directly, the isoxazoline-fused chlorins **79a–c** due to the spontaneous elimination of silanol from the intermediate *N*-silyloxyisoxazolidine cycloadducts **78a–c**. The obtained yields of the propyl and pentyl derivatives were quite low (16% and 18%, respectively), but the methyl ester derivative **79c** was obtained in a reasonable yield (34%). No bisaddition was observed in these reactions. Similar reactions using the less electron-deficient *meso*-tetrakis(3,5-difluorophenyl)porphyrin as dipolarophile yielded only traces of the desired chlorin, while with TPP no product was detected.



**Scheme 14.** Synthesis of isoxazoline-fused chlorins from porphyrin **9** and silyl nitronates.

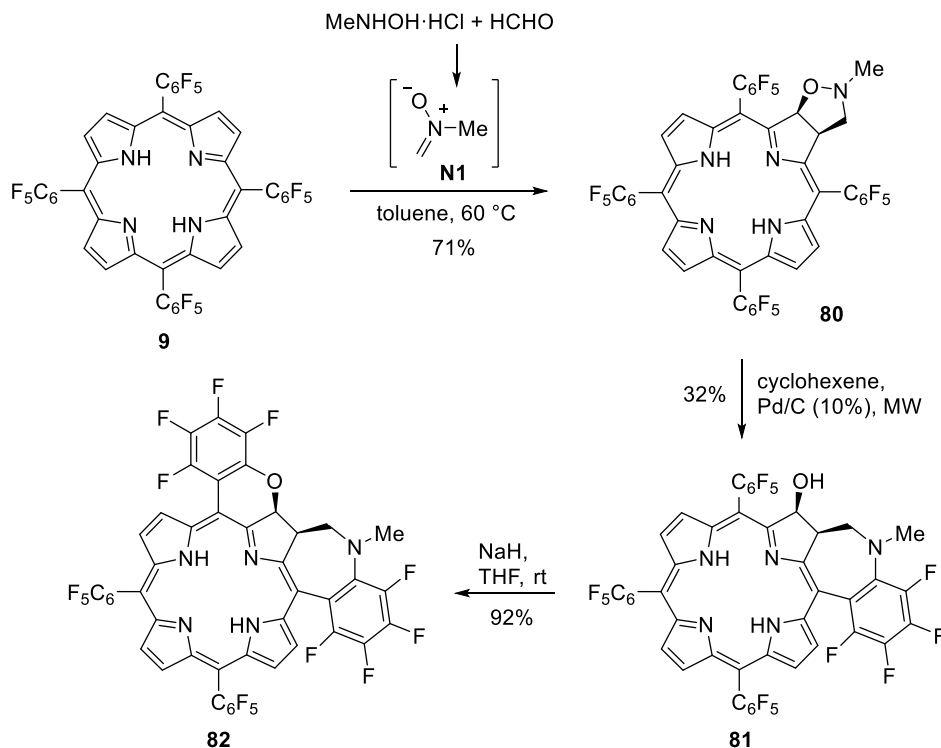
### 3.4. Reaction of porphyrins with nitrones

The 1,3-dipolar cycloaddition of porphyrins with nitrones gives isoxazolidine-fused chlorins,<sup>80</sup> valuable compounds for a range of applications, namely for PDT. An interesting study showed that the isoxazolidine-fused chlorins are also useful precursors to other porphyrin derivatives bearing extended exocyclic systems, as illustrated in

#### Scheme 15.<sup>81</sup>

The isoxazolidine-fused chlorin **80**, prepared from the reaction of *meso*-tetrakis(pentafluorophenyl)porphyrin (**9**) with *N*-methyl nitronone **N1** (generated *in situ* from *N*-methyl hydroxylamine hydrochloride and paraformaldehyde), was submitted to a microwave-assisted palladium-catalyzed hydrogenation transfer with cyclohexene that led to the cleavage of the isoxazolidine N–O bond (

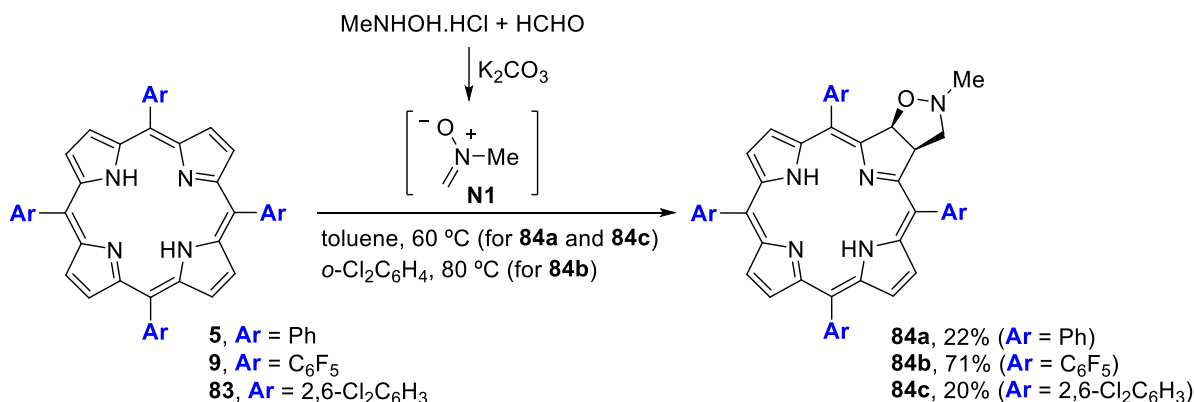
Scheme 15). The initially formed secondary amine function that resulted from the isoxazolidine ring-opening underwent a spontaneous nucleophilic aromatic substitution of the *o*-F atom of the adjacent aryl ring and led to the mono-annulated chlorin **81** in 32% yield. Further treatment of **81** with NaH induced a second intramolecular nucleophilic aromatic substitution generating the bis-annulated chlorin **82**. The final chlorin derivative, that comprises a 2,3-dihydro-1*H*-benzo[*b*]azepine ring system and a 2*H*-pyran ring, exhibited an unusual asymmetry and displayed a strong absorption band centered at 664 nm.



**Scheme 15.** Synthesis of isoxazolidine-fused chlorin **80**, and further intramolecular nucleophilic aromatic substitution to afford mono- (**81**) and bis-annulated chlorins (**82**).

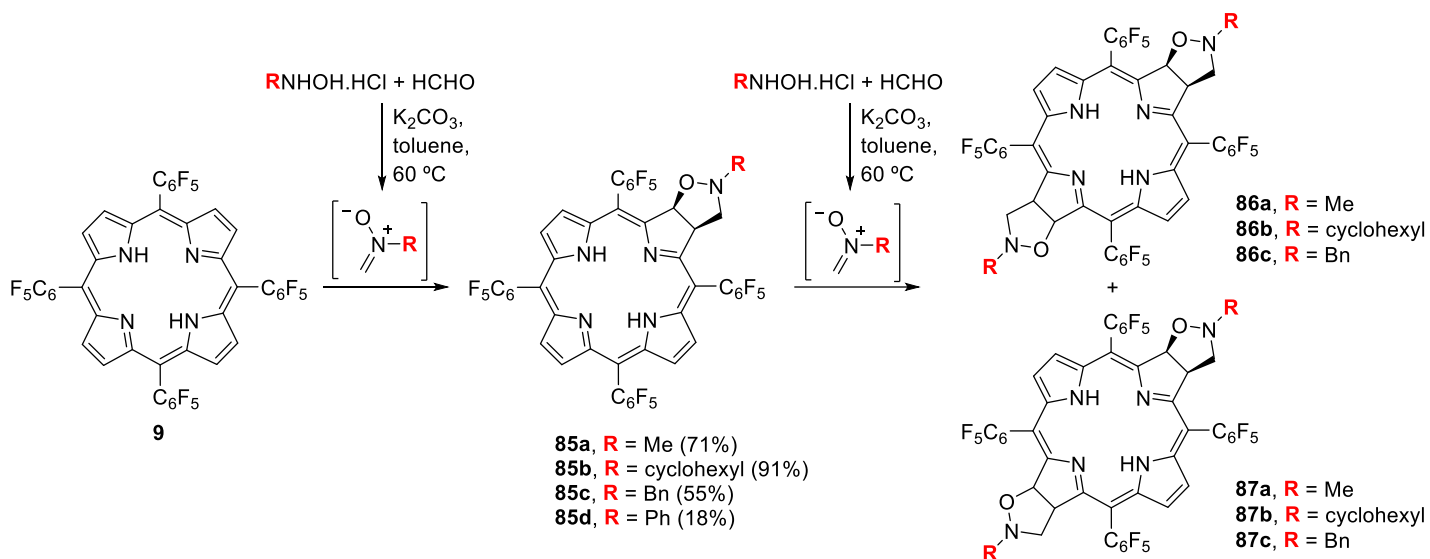
A recent study showed that the yields of the isoxazolidine-fused chlorins **84** vary greatly with the nature of the *meso*-aryl groups of the starting porphyrin.<sup>82</sup> While the reaction of *meso*-tetrakis(pentafluorophenyl)porphyrin (**9**) with *N*-methyl nitron **N1** afforded chlorin **84b** in 71% yield, similar reactions with *meso*-tetraphenylporphyrin (**5**) and *meso*-tetrakis(2,6-dichlorophenyl)porphyrin (**83**) gave the corresponding chlorins **84a** and **84c** in 22% and 20% yield, respectively (

Scheme 16).



**Scheme 16.** Reaction of *meso*-tetraarylporphyrins and *N*-methyl nitron **N1** afforded isoxazolidine-fused chlorins

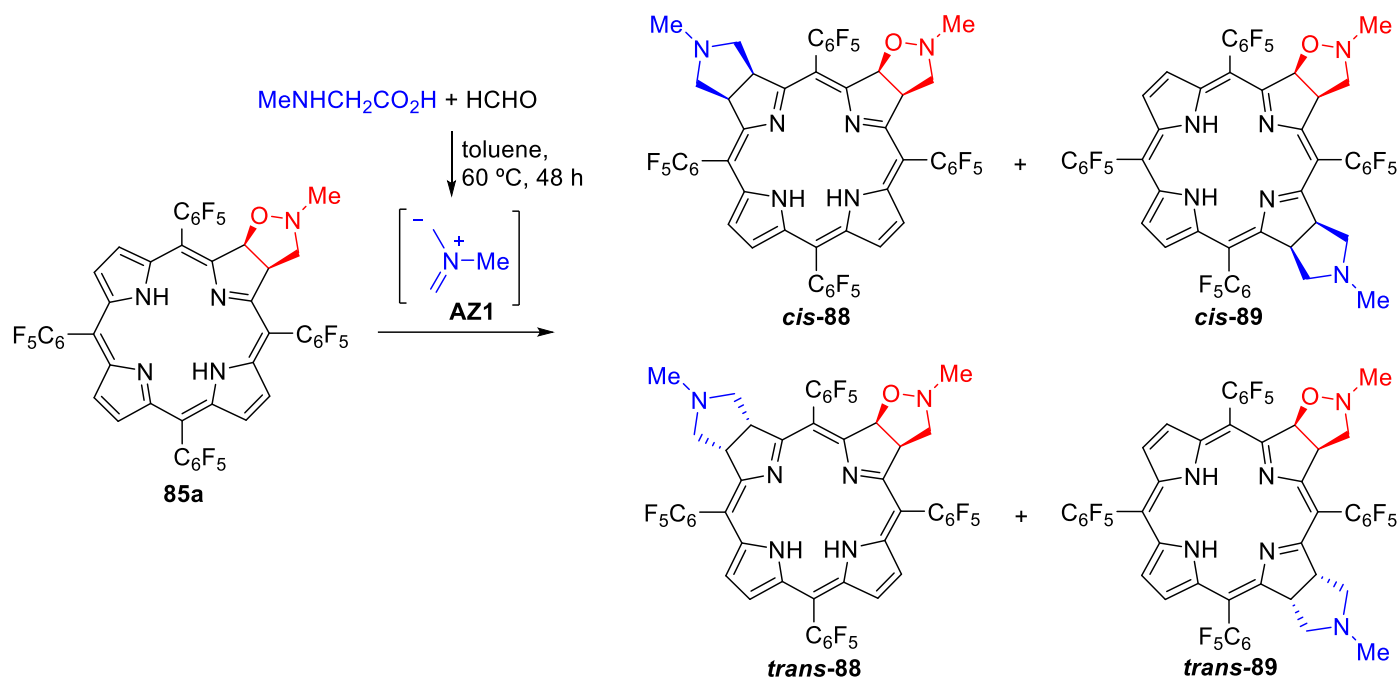
The same study also showed that the yields of the isoxazolidine-fused chlorins **85** vary greatly with the nature of the *N*-substituent group at the nitron, being the highest yield (91%) for *R* = cyclohexyl (Scheme 17).<sup>82</sup> Using the most reactive porphyrin (**9**) and the most reactive nitrones, bacteriochlorin-type bisadducts **86** and **87** were also obtained, albeit in low yields (Scheme 17).



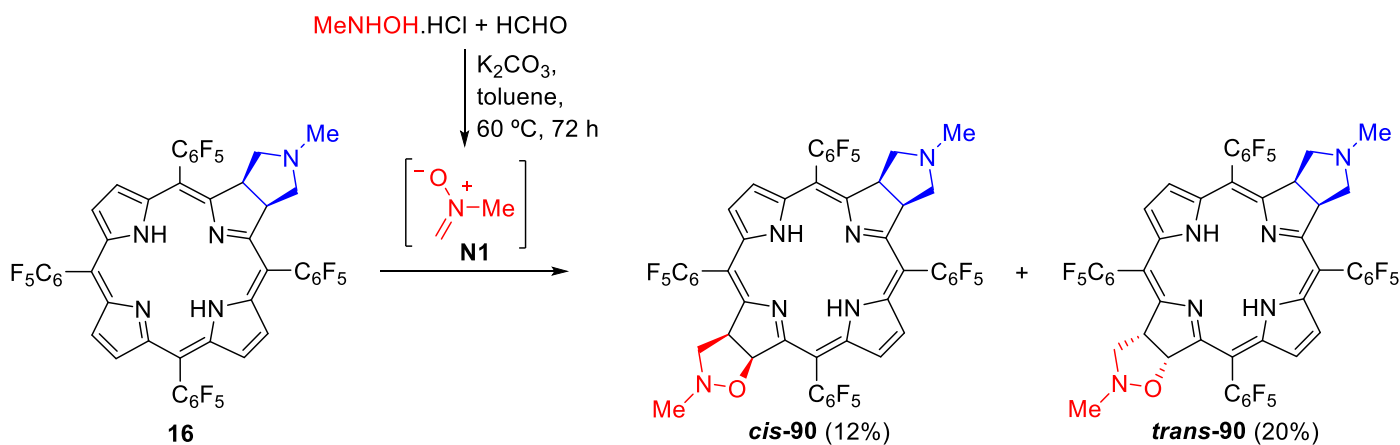
**Scheme 17.** Chlorins **85** and bacteriochlorins **86** and **87** synthesized by reaction of porphyrin **9** with various nitrones.

The synthesis of mixed bisadducts was also considered in the previous study.<sup>82</sup> The obtained experimental results confirmed that the selectivity of the bisaddition reactions can be set to provide selectively isobacteriochlorins or bacteriochlorins simply by reversing the sequence of reactions of a porphyrin with two different 1,3-dipolar species. In fact, the reaction of porphyrin **9** with nitron **N1**, followed by the reaction of resulting chlorin **85a** with azomethine ylide **AZ1** gave the isobacteriochlorins **88** and **89** (as a mixture of the four possible isomers) (

Scheme 18). However, the initial addition of the azomethine ylide to porphyrin **9** followed by the addition of nitron **N1** to the resulting chlorin **16**, led to the selective formation of bacteriochlorins **90** (Scheme 19).



**Scheme 18.** Synthesis of mixed bisadducts: reaction of the isoxazolidine-fused chlorin **85a** with an azomethine ylide.

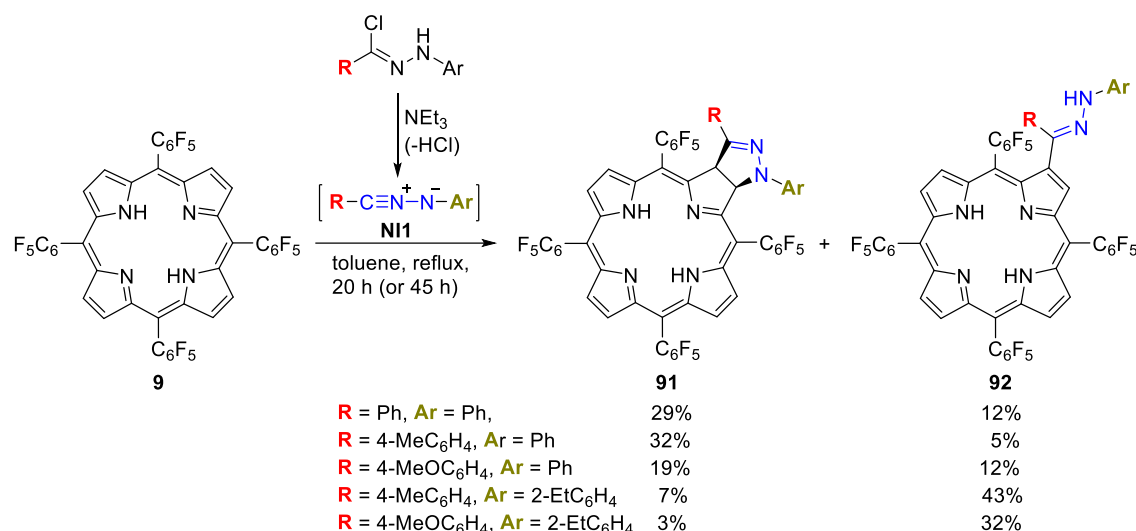


**Scheme 19.** Synthesis of mixed bisadducts: reaction of the pyrrolidine-fused chlorin **16** with a nitron.

### 3.5. Reaction of porphyrins with nitrile imines

The reactions of porphyrins with nitrile imines leads to pyrazoline-fused chlorins.<sup>83</sup> This type of reaction was studied using porphyrin **9** and nitrile imines **NI1** (generated *in situ* from functionalized  $\alpha$ -chlorohydrazone derivatives and NEt<sub>3</sub> or DABCO) under various experimental conditions. Unfortunately, the expected pyrazoline-fused chlorins **91** were obtained in low yields (Scheme 20).<sup>84</sup> In these reactions, porphyrin derivatives **92** were also formed and, in some cases, they are the main products. Best yields for cycloadducts **91** were obtained when Ar = Ph and R = Ph, 4-MeC<sub>6</sub>H<sub>4</sub> or 4-MeOC<sub>6</sub>H<sub>4</sub> (29%, 32% and 19% yield, respectively). The presence of an *o*-ethyl group on the *N*-aryl ring (Ar = 2-EtC<sub>6</sub>H<sub>4</sub>) led to a decrease of the yield of **91** to 7%, probably due to steric hindrance. In those cases, the formation of derivatives **92** prevail, being isolated in 43% (R = 4-MeC<sub>6</sub>H<sub>4</sub>) or 32% yield (R = 4-MeOC<sub>6</sub>H<sub>4</sub>). On the other hand, nitro substituents at the *N*-aryl ring suppress the reaction – no products were isolated when Ar = 4-NO<sub>2</sub>C<sub>6</sub>H<sub>4</sub> or 2,4-(NO<sub>2</sub>)<sub>2</sub>C<sub>6</sub>H<sub>3</sub>. Of note is that pyrazoline-fused chlorins **92**

display a strong absorption band at long wavelengths ( $\lambda_{\max} \approx 660$  nm) and may be useful dyes for biomedical applications.



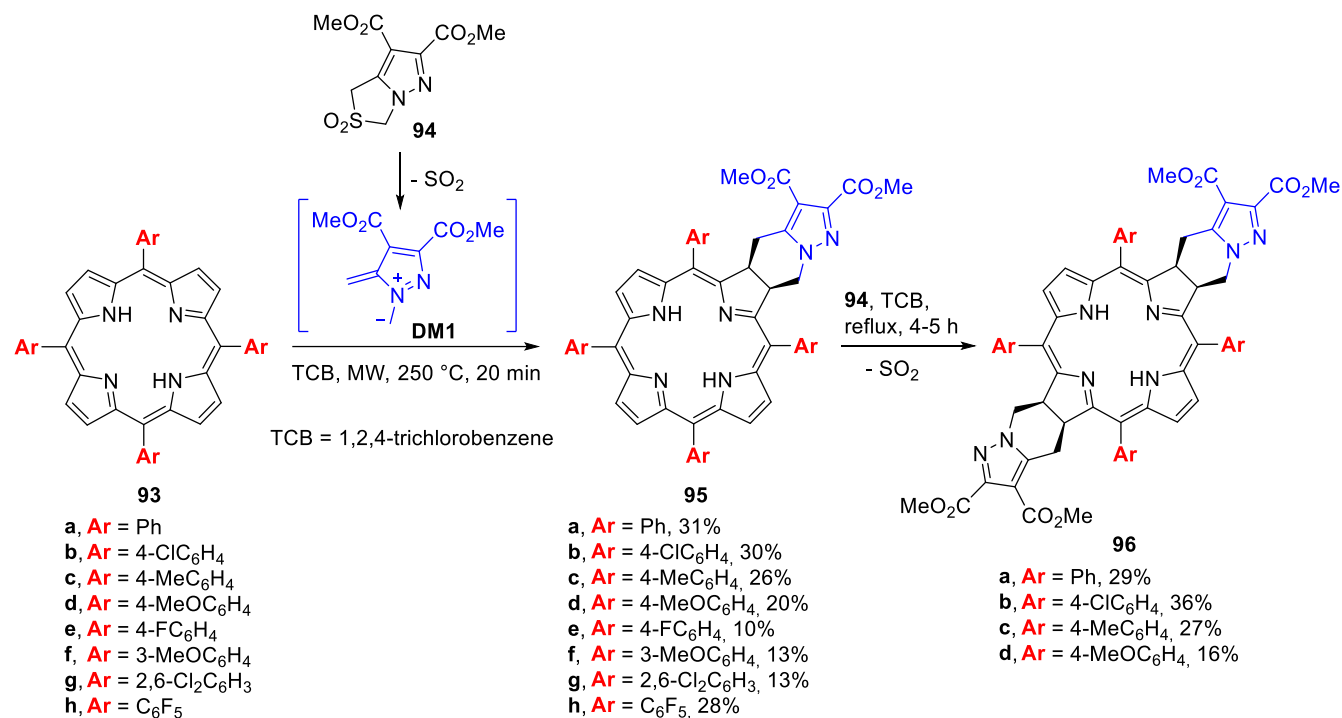
**Scheme 20.** Reaction of *meso*-tetrakis(pentafluorophenyl)porphyrin **9** with nitrile imines.

## 4. Other cycloadditions

### 4.1. Reaction of porphyrins with diazafulvenium methides

The diazafulvenium methide **DM1**, generated by thermal extrusion of  $\text{SO}_2$  from 2,2-dioxo-1*H*,3*H*-pyrazolo[1,5-*c*][1,3]thiazole **94**, reacts with *meso*-tetraarylporphyrins **93a-h** in  $[8\pi+2\pi]$  cycloadditions to give 4,5,6,7-tetrahydropyrazolo[1,5-*a*]pyridine-fused chlorin derivatives **95a-h** (Scheme 21).<sup>85</sup> The yield of these reactions is low or moderate, but most of the starting porphyrin is recovered. The reaction of chlorins **95a-d** with sulfone **94** in refluxing 1,2,4-trichlorobenzene afforded the corresponding bacteriochlorins **96a-d**. The best yield (36%) was obtained for bacteriochlorin **96b**, that was isolated as a single isomer with *cis* configuration (determined by X-ray crystallography). Chlorins **95** and bacteriochlorins **96** exhibit absorption spectra with a long wavelength absorption band with a maximum at *ca.* 649 nm and at *ca.* 727 nm, respectively. Compounds of these types are thus potentially useful for biomedical applications.





**Scheme 21.** Synthesis of chlorins **95** and bacteriochlorins **96**.

It has been recently shown that chlorins **97**<sup>86</sup> and **98**<sup>85</sup> (

Figure **22**) are efficient photosensitizers for the PDT of cancer. *In vitro* PDT studies with the luminescent platinum(II) chlorin **97** showed that it is active against human melanoma, esophageal adenocarcinoma and bladder carcinoma cell lines and *in vivo* studies using a A375 melanoma mouse model proved that this chlorin is able to impair tumor growth and, importantly, allows for image guided cancer treatment.<sup>86</sup> Chlorin **98** also revealed to be an efficient PS against human melanoma and esophageal carcinoma cell lines, with IC<sub>50</sub> values in the nanomolar range (13 nM and 27 nM, respectively).<sup>85</sup>

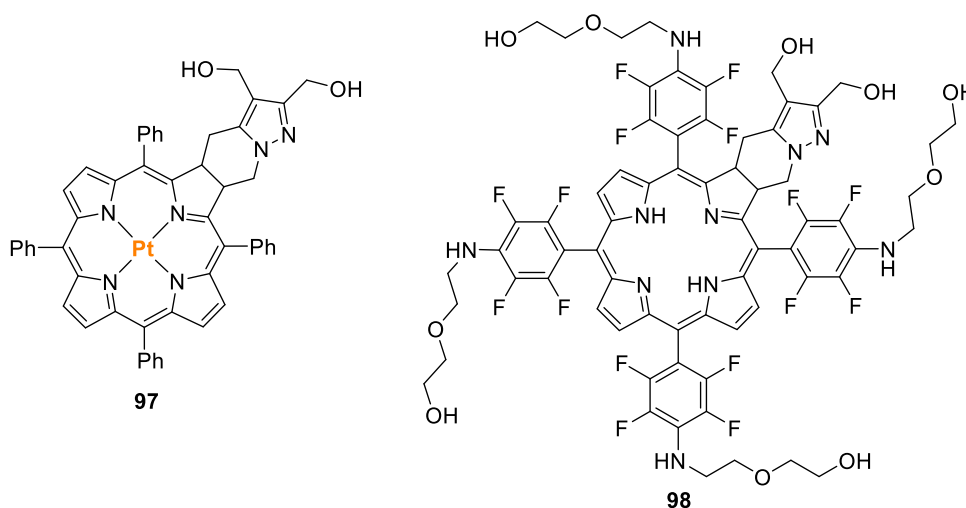


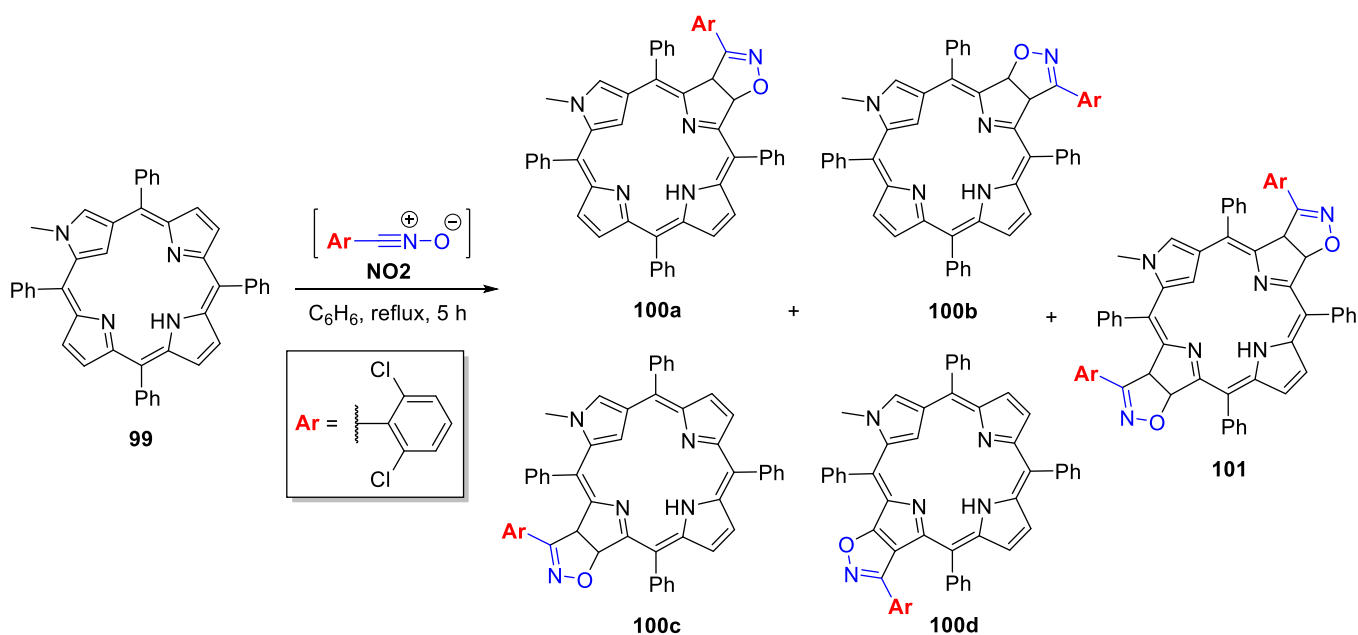
**Figure 22.** Structures of platinum(II) chlorin **97** and free base chlorin **98**.

## 5. Porphyrinoids cycloaddition reactions

The preparation of chlorin- and (iso)bacteriochlorin-like derivatives of other porphyrinoids has been receiving special attention from synthetic chemists due to their electronic, optical, and photophysical properties and potential applications such as photosensitizers in PDT. Some examples are described below.

The 2-methyl-*N*-confused porphyrin reacted with an excess of 2,6-dichlorobenzonitrile oxide **NO2** in refluxing benzene for 5 h to afford as main products a mixture of four monoadducts (29%) and one bis-adduct (20%) (Scheme 22). The reaction exhibited neither stereo- nor regioselectivity for the chlorin-type derivatives as the 2-aza-21-carbachlorins were obtained in a 55:27:13:5 molar ratio for **100a**:**100b**:**100c**:**100d**, respectively. However, the addition of a second 2,6-dichlorobenzonitrile oxide unit to the *N*-confused macrocycle allowed for the stereo- and regioselective synthesis of the bacteriochlorin-type derivative **101** bearing two isoxazoline-fused moieties.<sup>87</sup>

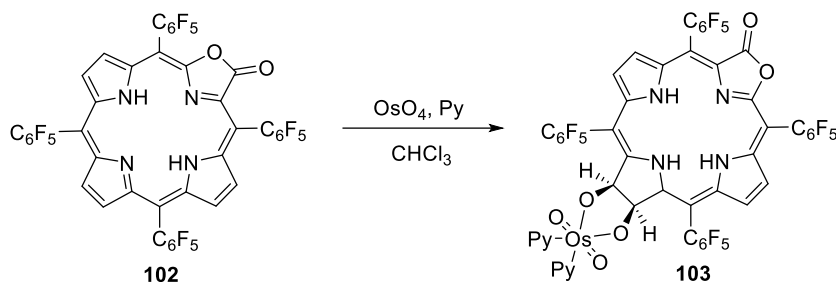
It is worth mentioning that the use of 2-*N*-methyl confused porphyrin **99** inhibits the dynamic process, which leads to the formation of two different *N*-confused tautomers due to the  $\pi$ -electron delocalization on the macrocycle, and consequently prevents the cycloaddition reaction at the pyrrolic positions in *trans*-position with respect to the *N*-confused pyrrole.

**Scheme 22.** Synthesis of 2-aza-21-carbachlorins **100a–d** and the corresponding bacteriochlorin **101** by reaction of 2-methyl-*N*-confused **99** porphyrin with nitrile oxide **NO2**.

Porpholactones are porphyrin analogs in which one or more of the  $\beta,\beta'$ -bonds have been replaced by a lactone unit through oxidation of the corresponding porphyrin derivative.<sup>88</sup> Hydroporpholactones can be prepared by reduction of  $\beta$ -pyrrolic positions with hydrazines. Treatment of the phenyl-*meso*-substituted porpholactone **102** with hydrazine gives the chlorin-like derivative with reduction of the opposite position

concerning the lactone-type unit.<sup>89</sup> On the other hand, the treatment of the *meso*-(pentafluorophenyl)-substituted analog with Woollins' reagent and PhMe<sub>2</sub>SiH affords the reduction of one of the adjacent positions.<sup>90</sup>

The reaction of porpholactone **102** with OsO<sub>4</sub> in CHCl<sub>3</sub> affords almost in quantitative yields the chlorin-type derivative **103** due to the osmylation reaction at the opposite pyrrolic position considering the pyrrolinone unit (Scheme 23). When the reaction was carried out with the Zn(II) or Pt(II) complexes of porpholactone **102** the transformation had taken place at the two pyrrole-type units adjacent to the oxazolone moiety. The corresponding metallo isobacteriochlorin-like osmate ester derivatives were isolated as an inseparable mixture in an approximate ratio of 2:1 in a 75% yield.<sup>91</sup>

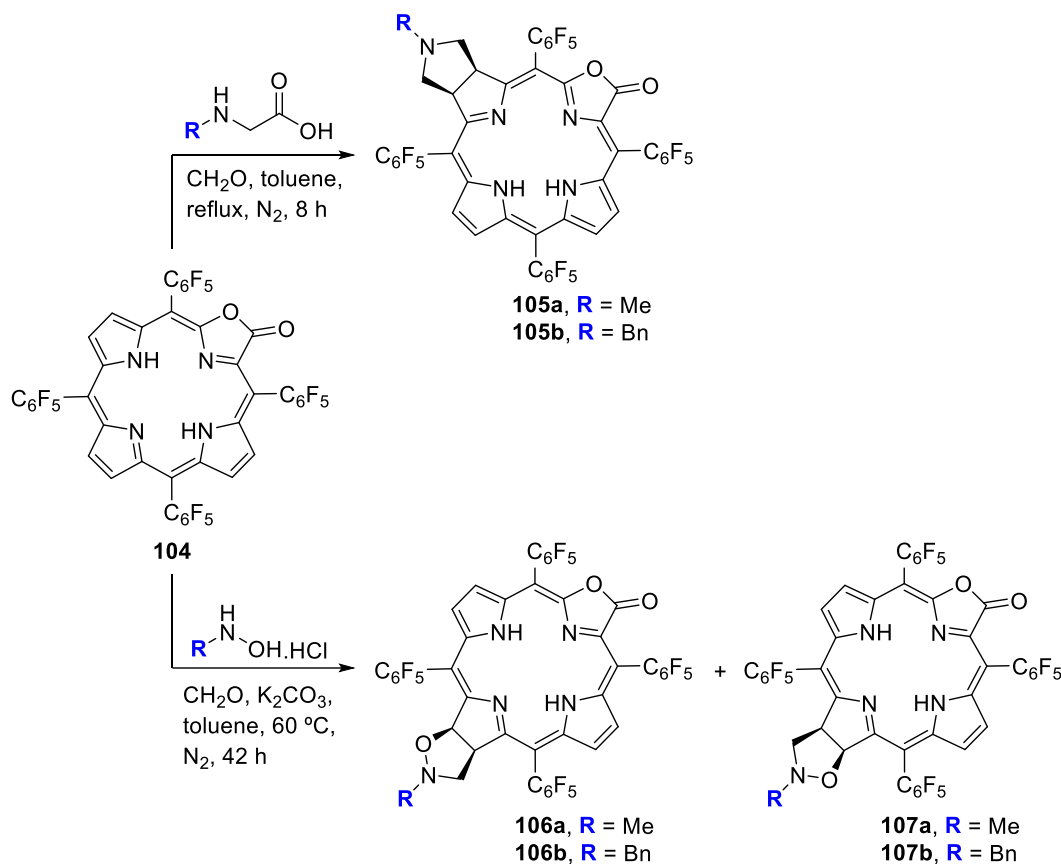


**Scheme 23.** Synthetic approaches to prepare hydroporpholactones.

It should be appreciated that the free base and metallo osmate ester derivatives are valuable intermediates to prepare bacteriodilactones and metalloisobacteriodilactones.<sup>91,92</sup>

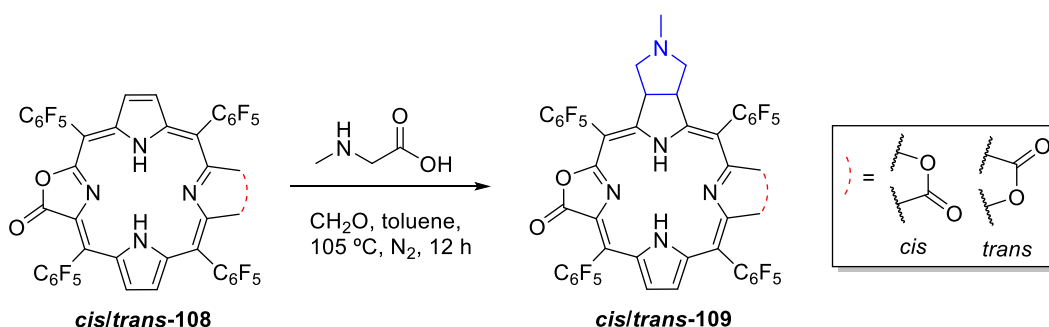
Tomé and co-workers studied the reactivity of free base porpholactone **104** with azomethine ylides and nitrones.<sup>93</sup> The reaction with azomethine ylides (generated *in situ* from the reaction of paraformaldehyde with *N*-methylglycine or *N*-benzylglycine) afforded the corresponding mono-adducts **105a** or **105b** in 85% and 43%, respectively (Scheme 24). The reaction is site-selective and occurs at an adjacent position of the lactone-like unit, affording new compounds with isobacteriochlorin-type electronic features.

The reaction with nitrones (generated *in situ* by basic treatment of *N*-methylhydroxylamine hydrochloride or *N*-benzylhydroxylamine hydrochloride and paraformaldehyde) also displays site-selectivity. However, the regioisomers **106** and **107** were formed from the cycloaddition reaction at the pyrrolic unit opposite to the lactone moiety in yields ranging from 8% to 22% (Scheme 24).<sup>93</sup>



**Scheme 24.** 1,3-Dipolar cycloadditions of porpholactone **104** with azomethine ylides and nitrones.

Zhang *et al.*<sup>94</sup> used **108** to prepare the *cis*- and *trans*-porphodilactone bacteriochlorin-like derivatives **109a,b** in 57% and 66% yield, respectively, using the 1,3-dipolar cycloaddition approach with azomethine ylide prepared from sarcosine and paraformaldehyde (Scheme 25).

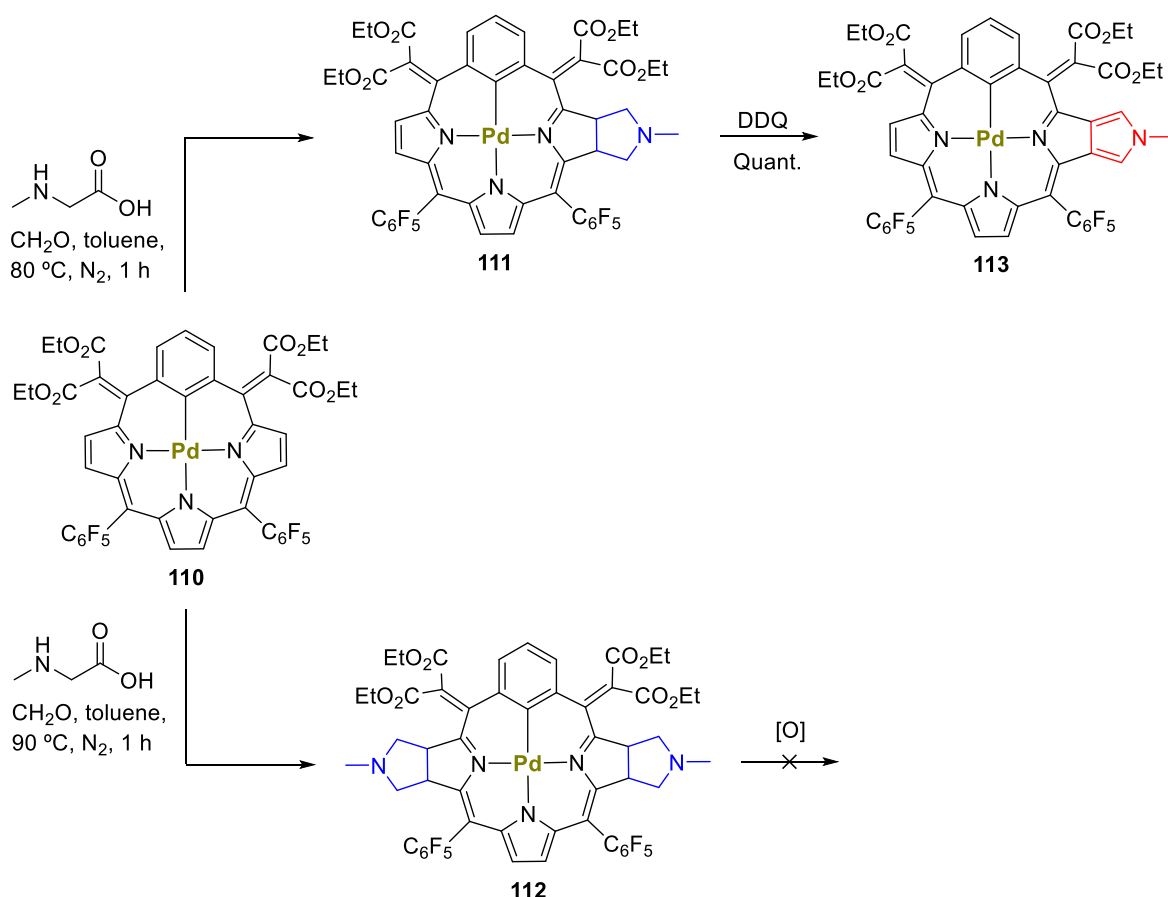


**Scheme 25.** Synthesis of porphodilactones bacteriochlorin-like **109a,b**.

Lee and co-workers<sup>95</sup> extended the 1,3-dipolar cycloaddition approach of azomethine ylides to prepare Pd(II) complex (benzi)chlorin **111** from the reaction of the precursor **110** and the azomethine ylide generated *in situ* at 90 °C in toluene for 1 h under  $N_2$ . The bacteriochlorin-type derivative **112** was also isolated as a diastereomeric mixture in 39% yield, being obtained as the chlorin-type analog but only in vestigial amounts. However, the authors found that the cycloaddition reaction, as well as the products formed, are temperature

dependent. By reducing the reaction temperature to 80 °C, it allowed for the mono-adduct to be isolated in comparable yield (37%) to the one obtained for the bis-adduct when the reaction was carried out at 90 °C (

Scheme 26).



**Scheme 26.** 1,3-Dipolar cycloaddition of Pd(II) complex (benzi)porphyrin **110** and azomethine ylide.

The oxidation of the chlorin-type derivative **111** with DDQ afforded the corresponding  $\pi$ -extended *N*-methylpyrrole-fused benziporphyrin **113**. Nevertheless, attempts to perform the oxidation of the bacteriochlorin-type derivative **112** were unsuccessful, leading to decomposition of the starting porphyrinoid (Scheme 26).

The same research group used a similar synthetic approach to prepare analogous pentaphyrin chlorin-type derivatives. The azomethine ylide (prepared *in situ* by reaction of sarcosine and paraformaldehyde) reacted with *meso*-diethylmalonylidene-(*m*-benzi)pentaphyrin affording the pentaphyrin chlorin-type analog **114** in 49% yield (

Figure 23).<sup>95</sup> After an oxidation step of the pyrrolidine ring, followed by reduction of the macrocycle with NaBH<sub>4</sub>, the resulting product was submitted to another 1,3-dipolar cycloaddition under the same conditions to afford the chlorin-type derivative **115** in 75% yield. The  $\pi$ -system delocalization can potentially be improved by submitting compound **115** to a new sequential oxidation and reduction protocol, affording a new derivative bearing two fused pyrrole-type moieties.

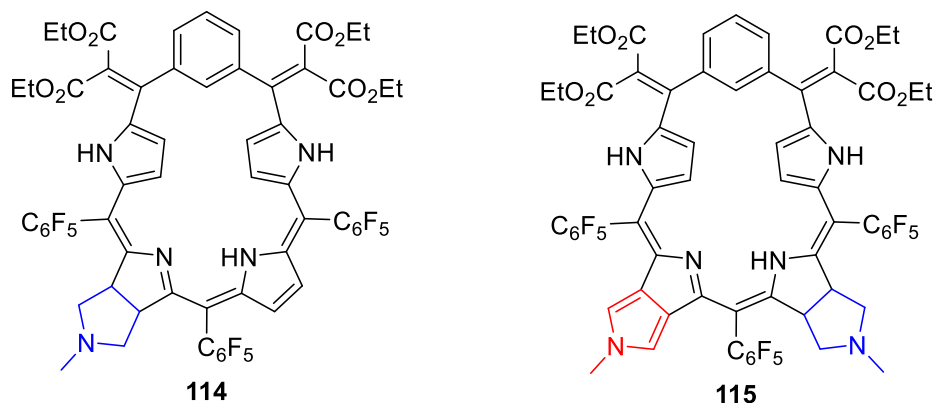
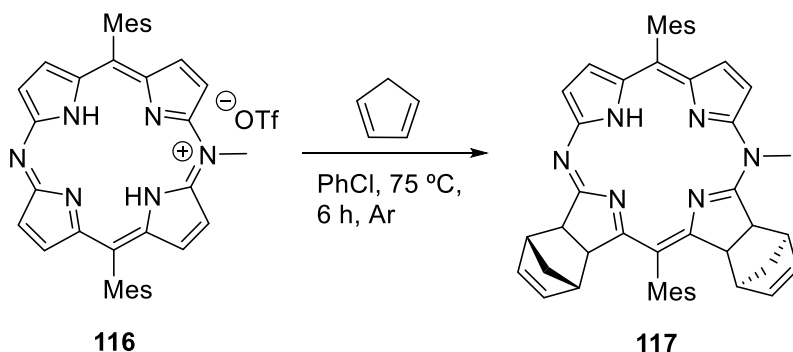


**Figure 23.** Structures of (*m*-benzi)pentaphyrin chlorin-type derivatives **114** and **115**.

These synthetic approaches also show the usefulness of the 1,3-dipolar cycloaddition procedure and synthesis of chlorin-type derivatives as templates to prepare  $\pi$ -extended porphyrinoids with improved photophysical properties.

The *N*-methyl-5,15-diazaporphyrinium derivative **116** reacted *via* a Diels-Alder reaction with a large excess of cyclopentadiene to afford regio- and stereoselectively the bis-adduct **117** in 53% yield (Scheme 27). The preparation of *N*-methyl-5,15-diazaporphyrinium cations significantly enhances the reactivity of porphyrin-related macrocycles as dienophiles through the substantial decrease of LUMO energy thereby improving the match with the HOMO energy level of cyclopentadiene.<sup>96</sup>



**Scheme 27.** Diels-Alder reaction of *N*-methyl-5,15-diazaporphyrinium cation **116** and cyclopentadiene.

## 6. Conclusions

This review covers the last ten years' literature data on the synthetic applicability of cycloaddition reactions to modify the structures of easily available porphyrinic macrocycles and making available other potential significant reduced porphyrin and porphyrin-type derivatives. The cycloaddition approach is a valuable tool in synthetic chemistry. Its application in the porphyrin field gives rise to novel reduced derivatives, namely chlorins and bacteriochlorins, which might demonstrate suitable and improved properties to be applied in several areas, including mainly in medicine as photosensitizers for the cancer photodynamic therapy. The recent development of cationic chlorins also allows for the consideration of photodynamic processes in the photoinactivation of microorganisms, including antibiotic resistant ones.

The versatility and usefulness of the cycloaddition reactions, particularly the 1,3-dipolar cycloadditions, has allowed a new synthetic route leading to dihydro- and tetrahydro-type derivatives where chlorins and bacteriochlorins, bearing substituents with different electronic behaviors in comparison with the starting porphyrin macrocycles, have a special significance.

The cycloaddition approach was also successfully extended to porphyrin-related macrocycles to prepare chlorin- or bacteriochlorin-like analogs with different features. Additionally, the new reduced compounds can be used as templates to prepare oxidized analogs, thus providing systems with  $\pi$ -system delocalization properties. It can be concluded that the development of new chlorins and bacteriochlorins with improved structural features and properties is a requirement to overcome the challenges brought by the several fields, mainly medicine, where such groups of novel derivatives provide avenues for potential applications.

## Acknowledgements

Thanks are due to the University of Aveiro and Fundação para a Ciência e a Tecnologia (FCT) for the financial support to LAQV-REQUIMTE UIDB/50006/2020) through national funds and, when applicable, co-financed by the FEDER, within the PT2020 Partnership Agreement, and to the Portuguese NMR Network. NMM Moura thanks his research contract (CDL-CTTRI-88- 89-97-ARH/2018) which is funded by national funds (OE), through FCT, in the scope of the framework contract foreseen in numbers 4, 5 and 6 of article 23, of the Law Decree 57/2016, of August 29, changed by Law 57/2017, of July 19. CJP Monteiro thanks the financial support of his research contract to the FCT project PREVINE (FCT-PTDC/ASP-PES/29576/2017).

## References

1. Dolphin, D. General Preface. In *The Porphyrins*; Academic: New York, 1978; pp xiii–xiv.  
<https://doi.org/10.1016/B978-0-12-220101-1.50005-6>
2. Willstätter, R. *Justus Liebigs Ann. Chem.* **1906**, 350, 48–82.  
<https://doi.org/10.1002/jlac.19063500103>
3. Woodward, R.B.; Ayer, W.A.; Beaton, J.M.; Bickelhaupt, F.; Bonnett, R.; Buchschacher, P.; Closs, G.L.; Dutler, H.; Hannah, J.; Hauck, F.P.; Itô, S.; Langemann, A.; Goff, E. Le; Leimgruber, W.; Lwowski, W.; Sauer, J.; Valenta, Z.; Volz, H. *J. Am. Chem. Soc.* **1960**, 82, 3800–3802.  
<https://doi.org/10.1021/ja01499a093>
4. Woodward, R.B.; Ayer, W.A.; Beaton, J.M.; Bickelhaupt, F.; Bonnett, R.; Buchschacher, P.; Closs, G.L.; Dutler, H.; Hannah, J.; Hauck, F.P.; Itô, S.; Langemann, A.; Le Goff, E.; Leimgruber, W.; Lwowski, W.; Sauer, J.; Valenta, Z.; Volz, H. *Tetrahedron* **1990**, 46, 7599–7659.  
[https://doi.org/10.1016/0040-4020\(90\)80003-Z](https://doi.org/10.1016/0040-4020(90)80003-Z)
5. Scheer, H. *An Overview of Chlorophylls and Bacteriochlorophylls: Biochemistry, Biophysics Functions and Applications*; Grimm, B., Porra, R.J., Rüdiger, W., Scheer, H., Eds.; 1st ed.; Springer Netherlands: Dordrecht, 2006; ISBN 978-1-4020-4515-8.
6. Banerjee, S.; Phadte, A.A. *ChemistrySelect* **2020**, 5, 11127–11144.  
<https://doi.org/10.1002/slct.202002644>
7. Dudkin, S. V; Makarova, E.A.; Lukyanets, E.A. *Russ. Chem. Rev.* **2016**, 85, 700–730.  
<https://doi.org/10.1070/RCR4565>

8. Acherar, S.; Colombeau, L.; Frochot, C.; Vanderesse, R. *Curr. Med. Chem.* **2015**, *22*, 3217–3254.  
<https://doi.org/10.2174/0929867322666150716115832>
9. Costa, J.I.T.; Tomé, A.C.; Neves, M.G.P.M.S.; Cavaleiro, J.A.S. *J. Porphyrins Phthalocyanines* **2011**, *15*, 1116–1133.  
<https://doi.org/10.1142/S1088424611004294>
10. Pineiro, M.; Serra, A.C.; Melo, T.M.V.D.P. e Synthetic Strategies to Chlorins and Bacteriochlorins. In *Handbook of Porphyrins: Chemistry, Properties and Applications*; Kaibara, A., Matsumara, G., Eds.; Nova Science Publishers, Inc.: New York, USA, 2012; pp 89–160 ISBN 978-1-62081-068-2.
11. Abrahamse, H.; Hamblin, M.R. New Photosensitizers for Photodynamic Therapy. *Biochem. J.* **2016**, *473*, 347–364.  
<https://doi.org/10.1042/BJ20150942>
12. Correia, J.H.; Rodrigues, J.A.; Pimenta, S.; Dong, T.; Yang, Z. *Pharmaceutics* **2021**, *13*, 1332.  
<https://doi.org/10.3390/pharmaceutics13091332>
13. Oliveira, K.; Momo, P.; Assis, F.; Ferreira, M.; Brocksom, T. *Curr. Org. Synth.* **2014**, *11*, 42–58.  
<https://doi.org/10.2174/15701794113106660085>
14. Huang, Y.-Y.; Luo, D.; Hamblin, M.R. *Curr. Org. Chem.* **2015**, *19*, 948–957.  
<https://doi.org/10.2174/1385272819666150303233445>
15. Gunaydin, G.; Gedik, M.E.; Ayan, S. *Front. Chem.* **2021**, *9*, 691697.  
<https://doi.org/10.3389/fchem.2021.691697>
16. Hopper, C.; Niziol, C.; Sidhu, M. *Oral Oncol.* **2004**, *40*, 372–382.  
<https://doi.org/10.1016/j.oraloncology.2003.09.003>
17. Bonnett, R. *Chemical Aspects of Photodynamic Therapy*; Gordon and Breach Science Publishers: Amsterdam: Netherlands, 2000.  
<https://doi.org/10.1201/9781482296952>
18. Yoon, I.; Li, J.Z.; Shim, Y.K. *Clin. Endosc.* **2013**, *46*, 7–23.  
<https://doi.org/10.5946/ce.2013.46.1.7>
19. Mashayekhi, V.; Hoog, C.O.; Oliveira, S. *J. Porphyrins Phthalocyanines* **2020**, 175–186.  
<https://doi.org/10.1142/S1088424619300180>
20. Grigg, R.; Johnson, A.W.; Sweeney, A. *Chem. Commun.* **1968**, 697–697.  
<https://doi.org/10.1039/C19680000697>
21. Inhoffen, H.H.; Jr., H.B.; Bliesener, K.-M. *Justus Liebigs Ann. Chem.* **1969**, *730*, 173–185.  
<https://doi.org/10.1002/jlac.19697300118>
22. Taniguchi, M.; Lindsey, J.S. *Chem. Rev.* **2017**, *117*, 344–535, doi:10.1021/ACS.CHEMREV.5B00696.  
<https://doi.org/10.1021/acs.chemrev.5b00696>
23. Cavaleiro, J.A.S.; Neves, M.G.P.M.S.; Tomé, A.C. *Arkivoc* **2003**, *2003*, 107–130.  
<https://doi.org/10.3998/ark.5550190.0004.e11>
24. Brückner, C.; Samankumara, L.; Ogikubo, J. *Synthesis of Bacteriochlorins and Isobacteriochlorins*; Kadish, K.M., Smith, K.M., R. Guillard, Eds.; World Scientific Publishing Co.: Singapore, 2012.  
[https://doi.org/10.1142/9789814335508\\_0003](https://doi.org/10.1142/9789814335508_0003)
25. Banala, S.; Sintic, P.; Kräutler, B. *Helv. Chim. Acta* **2012**, *95*, 211–220.  
<https://doi.org/10.1002/hlca.201100385>
26. Tomé, A.C.; Lacerda, P.S.S.; Neves, M.G.P.M.S.; Cavaleiro, J.A.S. *Chem. Commun.* **1997**, 1199–1200.  
<https://doi.org/10.1039/a702504a>
27. Silva, A.M.G.; Tomé, A.C.; Neves, M.G.P.M.S.; Cavaleiro, J.A.S. *Tetrahedron Lett.* **2000**, *41*, 3065–3068.



[https://doi.org/10.1016/S0040-4039\(00\)00336-1](https://doi.org/10.1016/S0040-4039(00)00336-1)

28. Silva, A.M.G.; Tomé, A.C.; Neves, M.G.P.M.S.; Cavaleiro, J.A.S.; Kappe, C.O. *Tetrahedron Lett.* **2005**, *46*, 4723–4726.

<https://doi.org/10.1016/j.tetlet.2005.05.047>

29. Peters, M.K.; Röhrich, F.; Näther, C.; Herges, R. *Org. Lett.* **2018**, *20*, 7879–7883.

<https://doi.org/10.1021/acs.orglett.8b03433>

30. Wellm, V.; Näther, C.; Herges, R. *J. Org. Chem.* **2021**, *86*, 9503–9514.

<https://doi.org/10.1021/acs.joc.1c00806>

31. Silva, A.M.G.; Tomé, A.C.; Neves, M.G.P.M.S.; Silva, A.M.S.; Cavaleiro, J.A.S. *Chem. Commun.* **1999**, 1767–1768.

<https://doi.org/10.1039/a905016g>

32. Silva, A.M.G.; Tomé, A.C.; Neves, M.G.P.M.S.; Silva, A.M.S.; Cavaleiro, J.A.S. *J. Org. Chem.* **2005**, *70*, 2306–2314.

<https://doi.org/10.1021/jo048349j>

33. Vinhado, F.S.; Gandini, M.E.F.; Iamamoto, Y.; Silva, A.M.G.; Simões, M.M.Q.; Neves, M.G.P.M.S.; Tomé, A.C.; Rebelo, S.L.H.; Pereira, A.M.V.M.; Cavaleiro, J.A.S. *J. Mol. Catal. A: Chem.* **2005**, *239*, 138–143.

<https://doi.org/10.1016/j.molcata.2005.06.014>

34. Pires, S.M.G.; Paula, R. De; Simões, M.M.Q.; Neves, M.G.P.M.S.; Santos, I.C.M.S.; Tomé, A.C.; Cavaleiro, J.A.S. *Catal. Commun.* **2009**, *11*, 24–28.

<https://doi.org/10.1016/j.catcom.2009.08.004>

35. Castro, K.A.D.F.; Pires, S.M.G.; Ribeiro, M.A.; Simões, M.M.Q.; Neves, M.G.P.M.S.; Schreiner, W.H.; Wypych, F.; Cavaleiro, J.A.S.; Nakagaki, S. *J. Colloid Interface Sci.* **2015**, *450*, 339–352.

<https://doi.org/10.1016/j.jcis.2015.03.028>

36. Aggarwal, A.; Bhupathiraju, N.V.S.D.K.; Farley, C.; Singh, S. *Photochem. Photobiol.* **2021**, <https://doi.org/10.1016/j.jcis.2015.03.028>

37. Jiménez-Osés, G.; García, J.I.; Silva, A.M.G.; Santos, A.R.N.; Tomé, A.C.; Neves, M.G.P.M.S.; Cavaleiro, J.A.S. *Tetrahedron* **2008**, *64*, 7937–7943.

<https://doi.org/10.1016/j.tet.2008.06.018>

38. Silva, A.M.G.; Tomé, A.C.; Neves, M.G.P.M.S.; Cavaleiro, J.A.S.; Perrone, D.; Dondoni, A. *Synlett* **2005**, *2005*, 0857–0859.

<https://doi.org/10.1055/s-2005-863736>

39. Maestrin, A.P.J.; Ribeiro, A.O.; Tedesco, A.C.; Neri, C.R.; Vinhado, F.S.; Serra, O.A.; Martins, P.R.; Iamamoto, Y.; Silva, A.M.G.; Tomé, A.C.; Neves, M.G.P.M.S.; Cavaleiro, J.A.S. *J. Braz. Chem. Soc.* **2004**, *15*, 923–930.

<https://doi.org/10.1590/S0103-50532004000600021>

40. Gryko, D.T.; Gałęzowski, M. *Org. Lett.* **2005**, *7*, 1749–1752.

<https://doi.org/10.1021/ol050327a>

41. Gałęzowski, M.; Gryko, D.T. *J. Org. Chem.* **2006**, *71*, 5942–5950.

<https://doi.org/10.1021/jo060545x>

42. De Assis, F.F.; De Souza, J.M.; Assis, B.H.K.; Brocksom, T.J.; De Oliveira, K.T. *Dyes Pigments* **2013**, *98*, 153–159.

<https://doi.org/10.1016/j.dyepig.2013.02.011>

43. Simões, J.C.S.; Sarpaki, S.; Papadimitroulas, P.; Therrien, B.; Loudos, G. *J. Med. Chem.* **2020**, *63*, 14119–14150.

<https://doi.org/10.1021/acs.jmedchem.0c00047>

44. Obata, M.; Hirohara, S.; Tanaka, R.; Kinoshita, I.; Ohkubo, K.; Fukuzumi, S.; Tanihara, M.; Yano, S. *J. Med. Chem.* **2009**, *52*, 2747–2753.

<https://doi.org/10.1021/jm8015427>

45. Hao, E.; Friso, E.; Miotto, G.; Jori, G.; Soncin, M.; Fabris, C.; Sibrian-Vazquez, M.; Vicente, M.G.H. *Org. Biomol. Chem.* **2008**, *6*, 3732–3740.

<https://doi.org/10.1039/b807836j>

46. Hirohara, S.; Obata, M.; Alitomo, H.; Sharyo, K.; Ando, T.; Tanihara, M.; Yano, S. *J. Photochem. Photobiol. B Biol.* **2009**, *97*, 22–33.

<https://doi.org/10.1016/j.jphotobiol.2009.07.007>

47. Hirohara, S.; Obata, M.; Alitomo, H.; Sharyo, K.; Ando, T.; Yano, S.; Tanihara, M. *Bioconjugate Chem.* **2009**, *20*, 944–952.

<https://doi.org/10.1021/bc800522y>

48. Singh, S.; Aggarwal, A.; Thompson, S.; Tomé, J.P.C.; Zhu, X.; Samaroo, D.; Vinodu, M.; Gao, R.; Drain, C.M. *Bioconjugate Chem.* **2010**, *21*, 2136–2146.

<https://doi.org/10.1021/bc100356z>

49. Tanaka, M.; Kataoka, H.; Mabuchi, M.; Sakuma, S.; Takahashi, S.; Tujii, R.; Akashil, H.; OHI, H.; Yano, S.; Morita, A.; Joh, T. *Anticancer Res.* **2011**, *31*, 763–769.

50. De Souza, J.M.; De Assis, F.F.; Carvalho, C.M.B.; Cavaleiro, J.A.S.; Brocksom, T.J.; De Oliveira, K.T. *Tetrahedron Lett.* **2014**, *55*, 1491–1495.

<https://doi.org/10.1016/j.tetlet.2014.01.049>

51. Terao, Y.; Kotaki, H.; Imai, N.; Achiwa, K. *Chem. Pharm. Bull.* **1985**, *33*, 896–898.

<https://doi.org/10.1248/cpb.33.896>

52. Padwa, A.; Dent, W. J. *Org. Chem.* **1987**, *52*, 235–244.

<https://doi.org/10.1021/jo00378a013>

53. Aggarwal, A.; Thompson, S.; Singh, S.; Newton, B.; Moore, A.; Gao, R.; Gu, X.; Mukherjee, S.; Drain, C.M. *Photochem. Photobiol.* **2014**, *90*, 419–430.

<https://doi.org/10.1111/php.12179>

54. Narumi, A.; Tsuji, T.; Shinohara, K.; Yamazaki, H.; Kikuchi, M.; Kawaguchi, S.; Mae, T.; Ikeda, A.; Sakai, Y.; Kataoka, H.; Inoue, M.; Nomoto, A.; Kikuchi, J.I.; Yano, S. *Org. Biomol. Chem.* **2016**, *14*, 3608–3613.

<https://doi.org/10.1039/C6OB00276E>

55. Pereira, P.M.R.; Silva, S.; Bispo, M.; Zuzarte, M.; Gomes, C.; Girão, H.; Cavaleiro, J.A.S.; Ribeiro, C.A.F.; Tomé, J.P.C.; Fernandes, R. *Bioconjugate Chem.* **2016**, *27*, 2762–2769.

<https://doi.org/10.1021/acs.bioconjchem.6b00519>

56. Gonzales, J.; Bhupathiraju, N.V.S.D.K.; Perea, W.; Chu, H.; Berisha, N.; Bueno, V.; Dodic, N.; Rozenberg, J.; Greenbaum, N.L.; Drain, C.M. *Chem. Commun.* **2017**, *53*, 3773–3776.

<https://doi.org/10.1039/C7CC01265A>

57. Gonzales, J.; Bhupathiraju, N.V.S.D.K.; Hart, D.; Yuen, M.; Sifuentes, M.P.; Samarxhiu, B.; Maranan, M.; Berisha, N.; Batteas, J.; Drain, C.M. *J. Org. Chem.* **2018**, *83*, 6307–6314.

<https://doi.org/10.1021/acs.joc.8b00169>

58. Hernández-Gil, J.; Lewis, J.S.; Reiner, T.; Drain, C.M.; Gonzales, J. *Chem. Commun.* **2020**, *56*, 12608–12611.

<https://doi.org/10.1039/D0CC05494A>

59. Gonzales, J.; Hernández-Gil, J.; Wilson, T.C.; Adilbay, D.; Cornejo, M.; Franca, P.D. de S.; Guru, N.; Schroeder, C.I.; King, G.F.; Lewis, J.S.; Reiner, T. *Mol. Pharm.* **2021**, *18*, 940–951.

<https://doi.org/10.1021/acs.molpharmaceut.0c00946>

60. Ol'shevskaya, V.A.; Kononova, E.G.; Zaitsev, A. V. *Beilstein J. Org. Chem.* **2019**, *15*, 2704–2709.

<https://doi.org/10.3762/bjoc.15.263>

61. Castro, K.A.D.F.; Ramos, L.; Mesquita, M.; Biazotto, J.C.; Moura, N.M.M.; Mendes, R.F.; Almeida Paz, F.A.; Tomé, A.C.; Cavaleiro, J.A.S.; Simões, M.M.Q.; Faustino, M.A.F.; Jager, A.V.; Nakagaki, S.; P.M.S. Neves, M.G.; da Silva, R.S. *ACS Appl. Bio Mater.* **2021**, *4*, 4925–4935.

<https://doi.org/10.1021/acsabm.1c00218>

62. Mesquita, M.Q.; Ferreira, A.R.; Neves, M.G.P.M.S.; Ribeiro, D.; Fardilha, M.; Faustino, M.A.F. *J. Photochem. Photobiol. B Biol.* **2021**, *223*, 112301.

<https://doi.org/10.1016/j.jphotobiol.2021.112301>

63. Sakamaki, Y.; Ozdemir, J.; Heidrick, Z.; Azzun, A.; Watson, O.; Tsuji, M.; Salmon, C.; Sinha, A.; Batta-Mpouma, J.; McConnell, Z.; Fugitt, D.; Du, Y.; Kim, J.W.; Beyzavi, H. *ACS Appl. Bio Mater.* **2021**, *4*, 1432–1440.

<https://doi.org/10.1021/acsabm.0c01324>

64. Costa, D.C.S.; Gomes, M.C.; Faustino, M.A.F.; Neves, M.G.P.M.S.; Cunha, Â.; Cavaleiro, J.A.S.; Almeida, A.; Tomé, J.P.C. *Photochem. Photobiol. Sci.* **2012**, *11*, 1905–1913.

<https://doi.org/10.1039/c2pp25113b>

65. Mesquita, M.Q.; Menezes, J.C.J.M.D.S.; Neves, M.G.P.M.S.; Tomé, A.C.; Cavaleiro, J.A.S.; Cunha, Â.; Almeida, A.; Hackbarth, S.; Röder, B.; Faustino, M.A.F. *Bioorg. Med. Chem. Lett.* **2014**, *24*, 808–812.

<https://doi.org/10.1016/j.bmcl.2013.12.097>

66. Mesquita, M.Q.; Menezes, J.C.J.M.D.S.; Pires, S.M.G.; Neves, M.G.P.M.S.; Simões, M.M.Q.; Tomé, A.C.; Cavaleiro, J.A.S.; Cunha, Â.; Daniel-Da-Silva, A.L.; Almeida, A.; Faustino, M.A.F. *Dyes Pigments* **2014**, *110*, 123–133.

<https://doi.org/10.1016/j.dyepig.2014.04.025>

67. Calmeiro, J.M.D.; Dias, C.J.; Ramos, C.I.V.; Almeida, A.; Tomé, J.P.C.; Faustino, M.A.F.; Lourenço, L.M.O. *Dyes Pigments* **2020**, *173*, 107410.

<https://doi.org/10.1016/j.dyepig.2019.03.021>

68. Santos, I.; Gamelas, S.R.D.; Vieira, C.; Faustino, M.A.F.; Tomé, J.P.C.; Almeida, A.; Gomes, A.T.P.C.; Lourenço, L.M.O. *Dyes Pigments* **2021**, *193*, 109557.

<https://doi.org/10.1016/j.dyepig.2021.109557>

69. Heredia, D.A.; Durantini, A.M.; Sarotti, A.M.; Gsponer, N.S.; Ferreyra, D.D.; Bertolotti, S.G.; Milanesio, M.E.; Durantini, E.N. *Chem. Eur. J.* **2018**, *24*, 5950–5961.

<https://doi.org/10.1002/chem.201800060>

70. Sobotta, L.; Sniechowska, J.; Ziental, D.; Długaszewska, J.; Potrzebowski, M.J. *Dyes Pigments* **2019**, *160*, 292–300.

<https://doi.org/10.1016/j.dyepig.2018.08.004>

71. Śniechowska, J.; Paluch, P.; Potrzebowski, M.J. *RSC Adv.* **2017**, *7*, 24795–24805.

<https://doi.org/10.1039/C7RA02217D>

72. Almeida, J.; Silva, A.M.N.; Rebelo, S.L.H.; Cunha-Silva, L.; Rangel, M.; De Castro, B.; Leite, A.; Silva, A.M.G. *New J. Chem.* **2018**, *42*, 8169–8179,

<https://doi.org/10.1039/C7NJ05165D>

73. Vargas, A.P.; Almeida, J.; Gámez, F.; Roales, J.; Queirós, C.; Rangel, M.; Lopes-Costa, T.; Silva, A.M.G.; Pedrosa, J.M. *Dyes Pigments* **2021**, *195*, 109721.

<https://doi.org/10.1016/j.dyepig.2021.109721>

74. Dommaschk, M.; Thoms, V.; Schütt, C.; Näther, C.; Puttreddy, R.; Rissanen, K.; Herges, R. *Inorg. Chem.* **2015**, *54*, 9390–9392.  
<https://doi.org/10.1021/acs.inorgchem.5b01756>
75. Ide, Y.; Kuwahara, T.; Takeshita, S.; Fujishiro, R.; Suzuki, M.; Mori, S.; Shinokubo, H.; Nakamura, M.; Yoshino, K.; Ikeue, T. *J. Inorg. Biochem.* **2018**, *178*, 115–124.  
<https://doi.org/10.1016/j.jinorgbio.2017.10.012>
76. Wyřębek, P.; Mikus, A.; Ostrowski, S. *Heterocycles* **2012**, *85*, 57–64.  
<https://doi.org/10.3987/COM-11-12347>
77. Betoni Momo, P.; Pavani, C.; Baptista, M.S.; Brocksom, T.J.; Thiago de Oliveira, K. *Eur. J. Org. Chem.* **2014**, *2014*, 4536–4547.  
<https://doi.org/10.1002/ejoc.201402227>
78. Liu, X.; Li, C.; Peng, X.; Zhou, Y.; Zeng, Z.; Li, Y.; Zhang, T.; Zhang, B.; Dong, Y.; Sun, D.; Cheng, P.; Feng, Y. *Dyes Pigments* **2013**, *98*, 181–189.  
<https://doi.org/10.1016/j.dyepig.2013.01.013>
79. O. Senge, M.; Moreau, M.; M. Ebrahim, M.; Ebrahim, M.M.; Moreau, M.; Senge, M.O. *Heterocycles* **2011**, *83*, 627–630.  
<https://doi.org/10.3987/COM-10-12125>
80. Silva, A.M.G.; Tomé, A.C.; Neves, M.G.P.M.S.; Silva, A.M.S.; Cavaleiro, J.A.S.; Perrone, D.; Dondoni, A. *Tetrahedron Lett.* **2002**, *43*, 603–605.  
[https://doi.org/10.1016/S0040-4039\(01\)02243-2](https://doi.org/10.1016/S0040-4039(01)02243-2)
81. Aguiar, A.; Leite, A.; Silva, A.M.N.; Tomé, A.C.; Cunha-Silva, L.; de Castro, B.; Rangel, M.; Silva, A.M.G. *Org. Biomol. Chem.* **2015**, *13*, 7131–7135.  
<https://doi.org/10.1039/C5OB00800J>
82. Almeida, J.; Aguiar, A.; Leite, A.; Silva, A.M.N.; Cunha-Silva, L.; De Castro, B.; Rangel, M.; Barone, G.; Tomé, A.C.; Silva, A.M.G. *Org. Chem. Front.* **2017**, *4*, 534–544.  
<https://doi.org/10.1039/C6QO00771F>
83. Moura, N.M.M.; Giuntini, F.; Faustino, M.A.F.; Neves, M.G.P.M.S.; Tomé, A.C.; Silva, A.M.S.; Rakib, E.M.; Hannioui, A.; Abouricha, S.; Röder, B.; Cavaleiroa, J.A.S. *Arkivoc* **2010**, (v), 24–33.  
<https://doi.org/10.3998/ark.5550190.0011.504>
84. Wyřębek, P.; Ostrowski, S. *Bull. Chem. Soc. Jpn.* **2012**, *85*, 1167–1174.  
<https://doi.org/10.1246/bcsj.20110408>
85. Pereira, N.A.M.; Laranjo, M.; Nascimento, B.F.O.; Simões, J.C.S.; Pina, J.; Costa, B.D.P.; Brites, G.; Braz, J.; Seixas de Melo, J.S.; Pineiro, M.; Botelho, M.F.; Pinho e Melo, T.M.V.D. *RSC Med. Chem.* **2021**, *12*, 615–627.  
<https://doi.org/10.1039/D0MD00433B>
86. Laranjo, M.; Aguiar, M.C.; Pereira, N.A.M.; Brites, G.; Nascimento, B.F.O.; Brito, A.F.; Casalta-Lopes, J.; Gonçalves, A.C.; Sarmiento-Ribeiro, A.B.; Pineiro, M.; Botelho, M.F.; Pinho e Melo, T.M.V.D. *Eur. J. Med. Chem.* **2020**, *200*.  
<https://doi.org/10.1016/j.ejmech.2020.112468>
87. Li, X.; Liu, B.; Yu, X.; Yi, P.; Yi, R.; Chmielewski, P.J. *J. Org. Chem.* **2012**, *77*, 2431–2440.  
<https://doi.org/10.1021/jo3000817>
88. Yu, Y.; Lv, H.; Ke, X.; Yang, B.; Zhang, J.-L. *Adv. Synth. Catal.* **2012**, *354*, 3509–3516.  
<https://doi.org/10.1002/adsc.201200720>
89. Akhigbe, J.; Haskoor, J.; Krause, J.A.; Zeller, M.; Brückner, C. *Org. Biomol. Chem.* **2013**, *11*, 3616–3628.

<https://doi.org/10.1039/c3ob40138c>

90. Yu, Y.; Furuyama, T.; Tang, J.; Wu, Z.Y.; Chen, J.Z.; Kobayashi, N.; Zhang, J.L. *Inorg. Chem. Front.* **2015**, *2*, 671–677.

<https://doi.org/10.1039/C5QI00054H>

91. Hewage, N.; Daddario, P.; Lau, K.S.F.; Guberman-Pfeffer, M.J.; Gascón, J.A.; Zeller, M.; Lee, C.O.; Khalil, G.E.; Gouterman, M.; Brückner, C. *J. Org. Chem.* **2019**, *84*, 239–256.

<https://doi.org/10.1021/acs.joc.8b02628>

92. Ning, Y.; Jin, G.Q.; Zhang, J.L. *Acc. Chem. Res.* **2019**, *52*, 2620–2633.

<https://doi.org/10.1021/acs.accounts.9b00119>

93. Cerqueira, A.F.R.; Snarskis, G.; Zurauskas, J.; Guieu, S.; Paz, F.A.A.; Tomé, A.C. *Molecules* **2020**, *25*, 2642.

<https://doi.org/10.3390/molecules25112642>

94. Yao, Y.; Rao, Y.; Liu, Y.; Jiang, L.; Xiong, J.; Fan, Y.J.; Shen, Z.; Sessler, J.L.; Zhang, J.L. *Phys. Chem. Chem. Phys.* **2019**, *21*, 10152–10162.

<https://doi.org/10.1039/C9CP01177C>

95. Park, D.; Jeong, S.D.; Ishida, M.; Lee, C.-H. *Chem. Commun.* **2014**, *50*, 9277–9280.

<https://doi.org/10.1039/C4CC04283B>

96. Chia, W.X.; Nishijo, M.; Kang, S.; Oh, J.; Nishimura, T.; Omori, H.; Longevial, J.F.; Miyake, Y.; Kim, D.; Shinokubo, H. *Chem. – A Eur. J.* **2020**, *26*, 2754–2760.

<https://doi.org/10.1002/chem.201905402>

This paper is an open access article distributed under the terms of the Creative Commons Attribution (CC BY) license (<http://creativecommons.org/licenses/by/4.0/>)